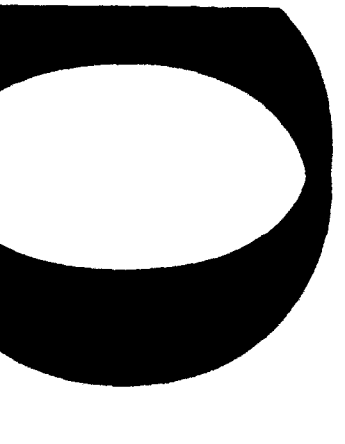

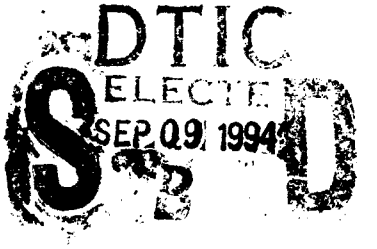

A Preliminary Study of the Airwake Model Used in an Existing SH-60B/FFG-7 Helicopter/Ship Simulation Program

Lincoln P. Erm

DEPARTMENT OF DEFENCE
DEFENCE SCIENCE AND TECHNOLOGY ORGANISATION

A Preliminary Study of the Airwake Model Used in an Existing SH-60B/FFG-7 Helicopter/Ship Simulation Program

Lincoln P. Erm

Aeronautical and Maritime Research Laboratory

ABSTRACT

Technical Report

The ship airwake model in a SH-60B/FFG-7 helicopter/ship simulation program is studied in detail. The airwake model is based on wind tunnel measurements obtained for another ship type, with geometric scaling applied to make it suitable for an FFG-7 frigate. Velocities over the flight deck of an FFG-7, predicted using the program, are compared with those obtained from full-scale tests on HMAS Darwin. Differences between predicted and measured velocities are often found to occur, indicating that the model used for prediction should be based on measurements for an FFG-7.

APPROVED FOR PUBLIC RELEASE

DSTO-TR-0015

DEPARTMENT OF DEFENCE

DEFENCE SCIENCE AND TECHNOLOGY ORGANISATION

Published by

DSTO Aeronautical and Maritime Research Laboratory
GPO Box 4331
Melbourne Victoria 3001 Australia

Telephone: (03) 626 7000
Fax: (03) 626 7999

AR No. 008-644
May 1994

APPROVED FOR PUBLIC RELEASE

CONTENTS

NOTATION

B	Airwake washout factor
f	Frequency
F	Airwake factor
F'	Multiplication factor
G	Turbulence gain factor
G_l	Turbulence altitude gain factor
H	Altitude of helicopter centre of gravity above sea level
H_F, H_{1F}	Height factors
I_{u_a}	Turbulence intensity for atmospheric turbulent velocity
L	Turbulence lag factor
N_{au}, N_{av}, N_{aw}	Scaled atmospheric white noise for xyz axes
N_{bu}, N_{bv}, N_{bw}	Scaled airwake white noise for xyz axes
R_{11}, R_{12}, R_{13}	Random numbers uniformly distributed between −1.0 and +1.0
S_u, S_v, S_w	Power spectral densities for xyz axes
t	Time
T	Turbulence level
U, V, W	Total simulation velocities for xyz axes
u_a, v_a, w_a	Turbulent velocities for the atmosphere for xyz axes
U_a, V_a, W_a	Mean-flow velocities for the atmosphere for xyz axes
u_b, v_b, w_b	Turbulent velocities for the airwake for xyz axes
U_b, V_b, W_b	Mean-flow velocities for the airwake for xyz axes
U_b^*, V_b^*, W_b^*	Incremental airwake velocities for xyz axes, obtained by combining mean-flow and turbulent components
u'_{xz}, u'_{yz}	Non-dimensionalized turbulent velocities in xz or yz planes for x'y'z' axes
U'_{xz}, U'_{yz}, V'_{xz}, W'_{xz}, W'_{yz}	Non-dimensionalized mean-flow velocities in xz or yz planes for x'y'z' axes
u'	Non-dimensional turbulent velocity for x' axis

U', V', W'	Non-dimensional mean-flow velocities for x'y'z' axes
U_{amb}	Mean velocity of the ambient wind in the atmosphere
U_{rel}	Velocity of the relative wind outside the airwake obtained using U_{amb} and U_{sh}
U_{sh}	Velocity of the ship
U_{tot}	Total wind velocity obtained by combining atmospheric and airwake velocities
x, y, z	Directions or distances in a coordinate system
xyz	Ship-carried vertical coordinate axes with z axis vertically down (see Fig. 2)
x'y'z'	Wind-over-deck coordinate axes with z' axis vertically down (see Fig. 2)
Δt_a, Δt_b	Frame time for subroutines ENVIR and BURBLE respectively
σ_u, σ_v, σ_w	Turbulence level factors for xyz axes
ψ	Direction of U_{rel} relative to x axis in ship-carried vertical coordinate system
ψ_{amb}	Direction of U_{amb} relative to x axis in ship-carried vertical coordinate system

Subscripts

a	Atmosphere
b	Airwake
h	Helicopter

Superscripts

i	ith time instant
'	Quantity associated with x'y'z' axes

1. INTRODUCTION

The Royal Australian Navy (RAN) operates Sikorsky S-70B-2 Seahawk helicopters from FFG-7 class frigates. To support the RAN with helicopter operations from these ships, a computer simulation program capable of modelling the complex interactions in the dynamic interface between the ship and helicopter is currently being developed. The program was obtained from the US Naval Air Warfare Center (NAWC) Aircraft Division at Patuxent River (previously known as the Naval Air Test Center) through The Technical Cooperation Program (TTCP) in 1987. It was in partially completed form with little documentation supplied. Although the simulation program obtained from NAWC was developed for the Sikorsky SH-60B Seahawk helicopter, it is planned to use it for the similar Sikorsky S-70B-2 Seahawk helicopter operated by the RAN. This report describes the program and its performance in predicting the airwake over the flight deck of an FFG-7 in circumstances for which actual measured data are available.

The SH-60B/FFG-7 simulation program is comprised of a number of different modules, each of which deals with a different aspect of the simulation. These are discussed in Ref. 1 and will only be briefly mentioned here. The Ship Motion Module gives the motion of the ship as a function of ship velocity, wavefront direction, and sea state. The Landing Gear Module, developed in Ref. 2, models undercarriage forces using non-linear equations which represent oleo deflection and tyre deformation. This module also models the Recovery Assist, Secure, and Traverse (RAST) system. The Airwake Module models the ambient atmospheric conditions as well as the ship airwake, which is the region of the flow field affected by the presence of the ship. Predicted velocities are assumed to act uniformly over the rotor and the helicopter is "fully porous" as far as the model is concerned. The rotor and vehicle aerodynamics of the SH-60B helicopter are modelled by the Aerodynamics Module. The Engine Module models the engines, either separately or together, as well as the transmission system of the helicopter. Pilot control inputs of collective and cyclic stick position, pedal movement, and throttle position are generated in the Pilot Module. The Control System Module models the mechanical flight controls and the Stability Augmentation System (SAS) feedback loops.

The helicopter behaviour during approach and landing is strongly influenced by the prevailing flow field over and around the flight deck in the wake of the FFG-7 superstructure. Because this flow field is modelled by the Airwake Module, it is important to investigate the accuracy of the module in representing the real flow.

Imperial units are adopted in this paper since (a) both the helicopter and ship referred to are built to imperial specifications in the US and (b) they are used exclusively by research workers in the US with whom AMRL is collaborating.

2. ORIGINS OF AIRWAKE MODEL

The airwake model used in the SH-60B/FFG-7 code was initially formulated by Fortenbaugh in 1977 (Ref. 3). The airwake model applied to a DE-1052 class ship (later redesignated as FF-1052) and was developed using Boeing-Vertol wind tunnel measurements, taken by Garnett in 1976 (Ref. 4), of the flow around a 1/50 scale model of an FF-1052 frigate. The frigate model was mounted on a ground board in a uniform free-stream having almost zero turbulence, which meant that an atmospheric turbulent boundary layer was not simulated in the experiments. It is indicated in Refs 5 and 6 that, strictly speaking, when the free-stream airflow to a ship is to be modelled in a wind tunnel, the mean speed profile, the turbulence intensity, the ratio of the turbulence length scale to the ship beam, and the spectrum function should be similar to the real flow. A wide range of velocities was measured by Garnett using an array of

hot-wire anemometer probes. Mean values and variances of velocities were determined for use in the data base in the airwake model. The turbulence model of Fortenbaugh is based on the assumption that full-scale turbulence may be accurately represented as second-order-filtered white noise, to which a mean velocity is added. White noise represents random turbulent fluid motion that has a uniform energy spectrum. The airwake model does not consider unsteady aerodynamic effects, so that phenomena such as the rapid change in location of separation points are disregarded.

In the late 1970s, Fortenbaugh extended his initial work so that the airwake model applied to a DD-963 destroyer (Refs 7 and 8). It was assumed that the superstructures of the DD-963 and FF-1052 were similar enough that geometric scaling could be used to make the measurements for the FF-1052 applicable to the DD-963. Such a procedure must be considered questionable, since the shapes of the two ships are markedly different with the flight deck of the FF-1052 being significantly closer to the stern than for the DD-963. In Fortenbaugh's modified airwake model, the random airwake components are generated using first-order-filtered white noise rather than second-order noise used earlier. This change, recommended by Nave (see Ref. 9), improves the accuracy of the model and reduces its complexity.

Boeing-Vertol wind tunnel measurements on a 1/80 scale model of a DD-963 destroyer were taken by Garnett in 1979 (Ref. 10). As for the earlier Boeing-Vertol data, velocities were measured using an array of hot-wire anemometer probes. It was understood that the measurements would be used directly to develop an airwake model for a DD-963, but the results have not yet been published.

In 1978, Nave (Ref. 9) formulated a refined version of the DE-1052 airwake model of Fortenbaugh (Ref. 3) as a result of additional analysis of the Boeing-Vertol data for the FF-1052 frigate (Ref. 4). Nave regulated the frequency content of the turbulence by varying the interval at which the Gaussian random number generators, used to generate fluctuating velocities, were called. The random number generators were called less frequently than the basic simulation time loop, and the resultant random number sequences were linearly interpolated to produce a smoothly varying number sequence at the loop time intervals. This procedure eliminated high frequency variations in the simulated turbulence. Using first order filtering and the random number interpolation scheme described, Nave found that there was reasonably good correspondence between spectra from the wind tunnel measurements and spectra from the simulated turbulence.

In 1983, Hanson (Ref. 11) incorporated the Nave random number modifications outlined above into the Fortenbaugh (Ref. 7) DD-963 airwake model. Simulated turbulence was produced both with and without the random number interpolation scheme of Nave, and spectra corresponding to the two cases were compared. Once again it was found that, using the interpolation scheme, there was a significant reduction in the high frequency content of spectra and essentially no change in the low frequency content. Hanson did not correlate the modified DD-963 airwake model with full-scale measurements, but he did carry out a small, non-rigorous, subjective correlation analysis of the airwake model by noting the opinions of pilots when they used the model in a piloted simulator. It was found that the simulated turbulence in the modified DD-963 airwake model was much too high and that a reduction of 60 to 70% of the total variances of the velocities was required to obtain a favourable opinion from the pilots. Hanson indicated that while this is a highly subjective way of verifying the airwake model, to this point it appears to have been the only attempt toward gaining some measure of confidence in the airwake model.

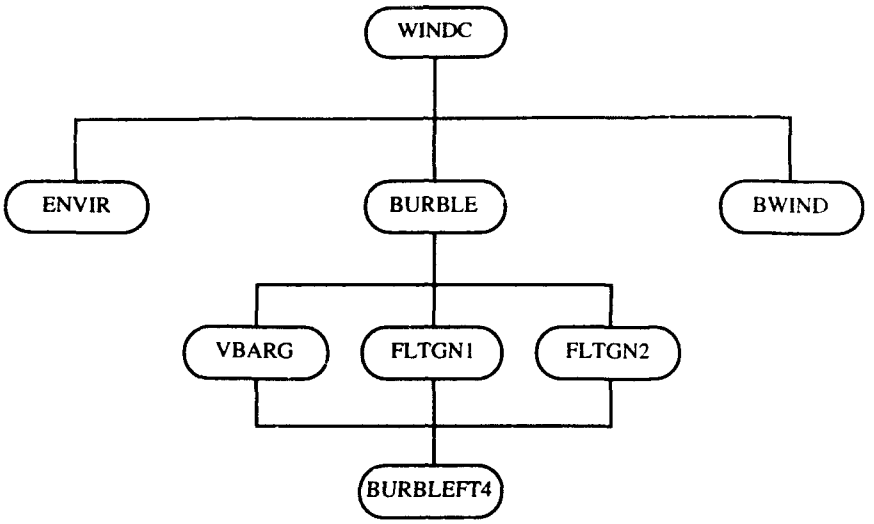

Fig. 1 Structure of Airwake Module

3. AIRWAKE MODULE

A block diagram of the structure of the Airwake Module is shown in Fig. 1. VBARG, FLTGN1, and FLTGN2 are interpolation routines which allow BURBLE to access data tables in BURBLEFT4. BWIND is believed to be an alternative model for the ambient atmosphere (ENVIR) and was not supplied, so calls to BWIND have been deleted.

The Airwake Module uses three coordinate systems. These are based on the earth, ship, and direction of the relative wind flowing over the ship deck (see Fig. 2). The origin of the ship-carried vertical coordinate system (referred to as the ship coordinate system) is located in the plane of the ship waterline, at the mid point of the fore-aft line of symmetry. The origin of the wind-over-deck coordinate system is located at the level of the flight deck, one-half hangar face width forward of the hangar face. For this system, the x axis is in the direction of the mean wind relative to the ship. The bullseye is the landing position pattern painted on the flight deck and its centre is 161.7 ft aft of the origin of the ship coordinate system.

Although the Airwake Module uses three coordinate systems, it is only velocities relative to the ship that are important for the present purpose. The ship coordinate system can be made to coincide with the earth coordinate system for the purposes of this study by having a ship heading North.

The computation of velocities using subroutines ENVIR, BURBLE, and WINDC will now be outlined. Fortran variables used in the Airwake Module, as well as corresponding symbols, are given in Appendix A. Fortran expressions used when determining velocities are given in Appendix B.

3.1 Subroutine ENVIR

Subroutine ENVIR computes both mean-flow and turbulent velocities for the three ship-coordinate directions for an ambient turbulent atmosphere. Inputs into subroutine ENVIR include the atmospheric wind speed, U_{amb}, and direction, ψ_{amb}.

Mean-flow velocities for the atmosphere, denoted by U_a, V_a, and W_a, in xyz axes, are determined by resolving U_{amb} as follows:

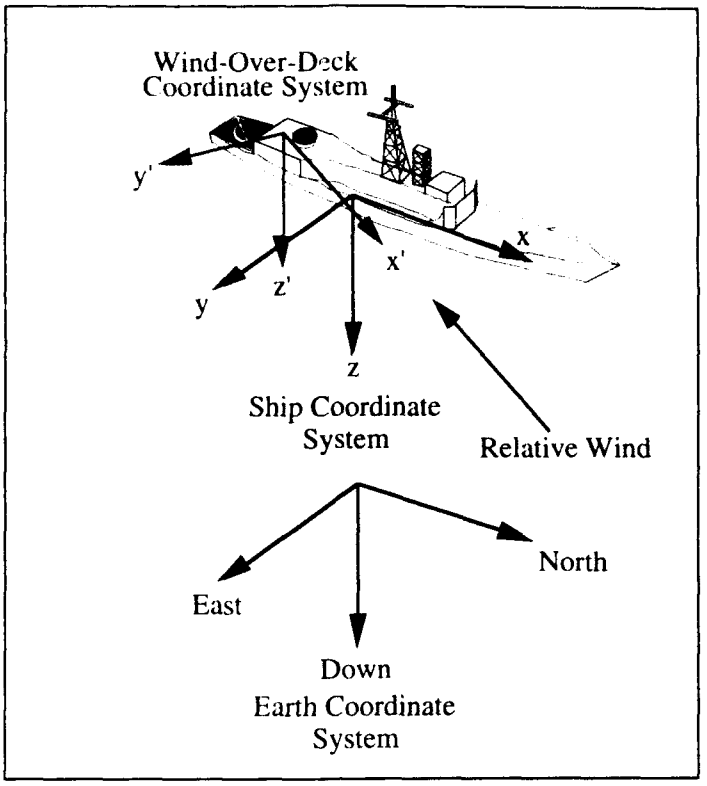

Fig. 2 Coordinate systems used in Airwake Module

$$U_a = -U_{amb} \cos \psi_{amb} \tag{1}$$

$$V_a = -U_{amb} \sin \psi_{amb} \tag{2}$$

$$W_a = 0 \tag{3}$$

U_{amb} and ψ_{amb} are shown in Fig. 3, which includes other velocities and flow angles to be referred to later. It is also possible to incorporate shear winds and deterministic time variations in the flow into the simulation by adding mean velocities associated with these perturbations to U_a, V_a, and W_a.

In xyz axes, the turbulent velocities for the atmosphere, u_a, v_a, and w_a, are determined using

$$\begin{bmatrix} u_a \\ v_a \\ w_a \end{bmatrix}^i = L_a \begin{bmatrix} u_a \\ v_a \\ w_a \end{bmatrix}^{(i-1)} + G \begin{bmatrix} N_{au} \\ N_{av} \\ N_{aw} \end{bmatrix} \tag{4}$$

where the superscript i corresponds to the ith time instant. As can be seen, u_a, v_a, and w_a are each determined by adding two distinct parts. The first part incorporates the lag factor, L_a, which is used to factor velocities from the previous time instant. The second part incorporates the turbulence gain factor, G, which is multiplied by random-number-dependent noise terms. In the mathematical study of time series, Equation 4 represents a simple autoregression (see

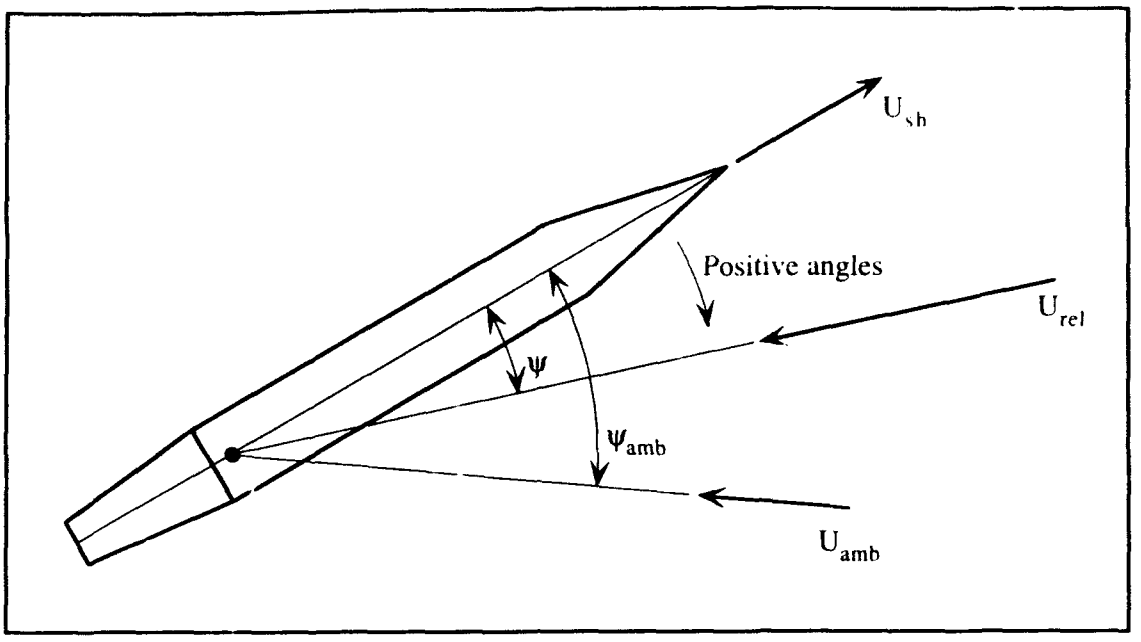

Fig. 3 Representation of velocities and flow angles

Ref. 14) in which the value of a variable at a given instant of time depends upon its values at previous instants of time as well as upon random components at previous instants of time. Equation 4 corresponds to a simplified representation of such a process since only terms up to time instant (i-1) are used.

In Equation 4, turbulent fluctuations are generated by the use of the noise terms which, for the atmosphere, are given by the following relationship:

$$\begin{bmatrix} N_{au} \\ N_{av} \\ N_{aw} \end{bmatrix} = T_a \begin{bmatrix} |R_{11}| R_{11}\ \sigma_u \\ |R_{12}| R_{12}\ \sigma_v \\ |R_{13}| R_{13}\ \sigma_w H_F \end{bmatrix} \tag{5}$$

N_{au}, N_{av}, and N_{aw} correspond to scaled white noise in xyz axes. R_{11}, R_{12}, and R_{13} are random numbers whose values can vary between -1.0 and +1.0. σ_u, σ_v, and σ_w are turbulence level factors for xyz axes, and T_a is the turbulence level for the atmosphere. The σ terms have a default value of 5.0 and T_a has a default value of 1.0. N_{au} and N_{av} do not vary with altitude, whereas N_{aw} can vary with altitude via the height factor, H_F, which is given by

$$H_F = 0.1 \qquad \text{for } H > 100.0 \text{ ft} \tag{6a}$$

$$H_F = 0.001\ H \qquad \text{for } H \leq 100.0 \text{ ft} \tag{6b}$$

where H is the height of the helicopter centre of gravity above sea level. In Ref. 12 (pp. 200-204) it is indicated that there is an initial increase in the vertical turbulence fluctuations with height up to between 100 and 200 m in a marine atmospheric boundary layer, which reflects the limiting influence of the sea surface on the intensity of vertical turbulent motion. It is also

indicated that the variations in the horizontal turbulence fluctuations with height are small. The model thus shows some consistency with this behaviour.

The turbulence intensity for u_a, the turbulent velocity for the atmosphere, is given by

$$I_{u_a} = \frac{(\overline{u_a^2})^{0.5}}{U_{amb}} \tag{7}$$

and similarly for v_a, and w_a. For heights greater than 100 ft and for a 35 knot relative wind, the turbulence intensities corresponding to u_a, v_a, and w_a were calculated to be about 0.004, 0.004, and 0.0004 respectively. While intensities corresponding to u_a and v_a are comparable with values given in Ref. 12, the intensity corresponding to w_a is much smaller. Removal of the height factor, H_F, (i.e. H_F set equal to 1.0 in Equation 6) gives an intensity for w_a of 0.004, which is comparable with the r an value over all heights in Ref. 12. A height factor of 1.0 is therefore used in the model predictions given in Section 4.

The turbulence gain factor, G, in Equation 4 is given by

$$G = (0.01\, U_{tot})^{0.5}\, G_1\, \Delta t_a \tag{8}$$

where U_{tot} is the total wind velocity obtained by combining atmospheric and airwake velocities. Δt_a is the frame time for subroutine ENVIR and has a value of 0.0667 second, i.e. the atmospheric model operates at 15 Hz. G can vary with altitude via the turbulence altitude gain factor, G_1, which is given by

$$G_1 = 1.0 \qquad \text{for } H > 100.0 \text{ ft} \tag{9a}$$

$$G_1 = 0.005\, H + 0.5 \qquad \text{for } H \le 100.0 \text{ ft} \tag{9b}$$

The turbulence lag factor for the atmosphere, L_a, in Equation 4 is given by

$$L_a = 1.0 - 0.01\, U_{tot}\, \Delta t_a \tag{10}$$

The airwake models of Fortenbaugh (Refs 3, 7, and 8), outlined in Section 2, do not include velocities due to atmospheric turbulence, and thus the models only describe ship-generated turbulence. This is presumably because the atmospheric turbulent boundary layer was not simulated in the Boeing-Vertol wind tunnel measurements (Ref. 4), upon which the airwake model is based. The code supplied to AMRL had previously been modified to include atmospheric turbulence, as described above.

3.2 Subroutine BURBLE

Subroutine BURBLE computes an incremental flow field for both mean-flow and turbulent velocities due to the presence of a ship for chosen operating conditions. The ship can be chosen to be either an FFG-7 'Oliver Hazard Perry' class frigate, a DD-963 'Spruance' class destroyer, or a CVN-68 'Nimitz' class carrier. The incremental flow field for the chosen ship is determined using one of two data bases of tabulated numbers within the program. One data base is for both the FFG-7 and the DD-963, and the other is for the CVN-68. The data base for both the FFG-7 and the DD-963 is based on data obtained from a 1/50 scale model of an

FF-1052 'Knox' class frigate, with geometric scaling used to apply the data base to either the FFG-7 or the DD-963. When using the data base for the CVN-68, geometric scaling is not used as the data in the data base correspond to this ship type.

The validity of applying the geometric scaling technique to the FFG-7 is questionable, since the shapes of the FF-1052 and the FFG-7 are markedly different. Side views of both these ships are shown to the same scale in Fig. 4. It can be seen that the hangar height on the FFG-7 is proportionately greater than that on the FF-1052. For the FF-1052, there is a lower deck behind the flight deck, whereas for the FFG-7 the flight deck extends almost to the end of the ship. In addition, the superstructure of the FF-1052 occupies a significantly smaller fraction of the ship width compared with the FFG-7 in the region forward of the hangar. Nevertheless, it was the only available option for the initial tests of the program for Australian purposes.

Inputs into subroutine BURBLE include ship speed and direction, wind speed and direction, and helicopter location in xyz axes. These variables are used to calculate the direction of the relative wind outside the airwake, as well as the coordinates of the helicopter centre of gravity in x'y'z' axes. Using these helicopter coordinates, as well as a geometric scaling factor, the geometrically-scaled helicopter location (x_h', y_h', z_h') in x'y'z' axes is computed for entry into the airwake data base for the FFG-7. The geometric scaling factor is given by the ratio of the maximum beam width of an FFG-7 to that of an FF-1052 (i.e. 0.9615).

Incremental airwake velocities, U_b^*, V_b^*, and W_b^*, in xyz axes, are determined by combining mean-flow components, U_b, V_b, and W_b, and turbulent components, u_b, v_b, and w_b, as follows:

$$\begin{bmatrix} U_b^* \\ V_b^* \\ W_b^* \end{bmatrix}^i = F \begin{bmatrix} U_b + u_b \\ V_b + v_b \\ W_b + w_b \end{bmatrix} + (1.0 - F) \begin{bmatrix} U_b^* \\ V_b^* \\ W_b^* \end{bmatrix}^{(i-1)} \tag{11}$$

Incremental airwake velocities are the perturbations to the flow field arising as a consequence of the presence of a ship. It can be seen that these velocities are weighted by their values from the previous time interval by using F, the airwake factor, which is a function of the helicopter location and can vary between 0.01 and 0.99.

Turbulent velocities for the airwake in xyz axes are determined using

$$\begin{bmatrix} u_b \\ v_b \\ w_b \end{bmatrix}^i = L_b \begin{bmatrix} u_b \\ v_b \\ w_b \end{bmatrix}^{(i-1)} + U_{rel}\, u' G \begin{bmatrix} N_{bu} \\ N_{bv} \\ N_{bw} \end{bmatrix} \tag{12}$$

which is a simple autoregression and has a form similar to Equation 4 for the atmosphere, but contains the additional variables U_{rel} and u'.

Before terms appearing in Equations 11 and 12 are discussed, it will first be necessary to give some details of the data base used when determining the incremental flow field. The data base consists of eight sets of tables, represented by the families of graphs shown in Fig. 5. These are for mean-flow velocities (Figs 5a, 5b, 5c, 5e, and 5f), the wind-over-deck direction (Fig. 5d), and turbulence velocities (Figs 5g and 5h). Table values are shown as solid circles. These are joined by straight-line segments to indicate the use of linear interpolation to determine

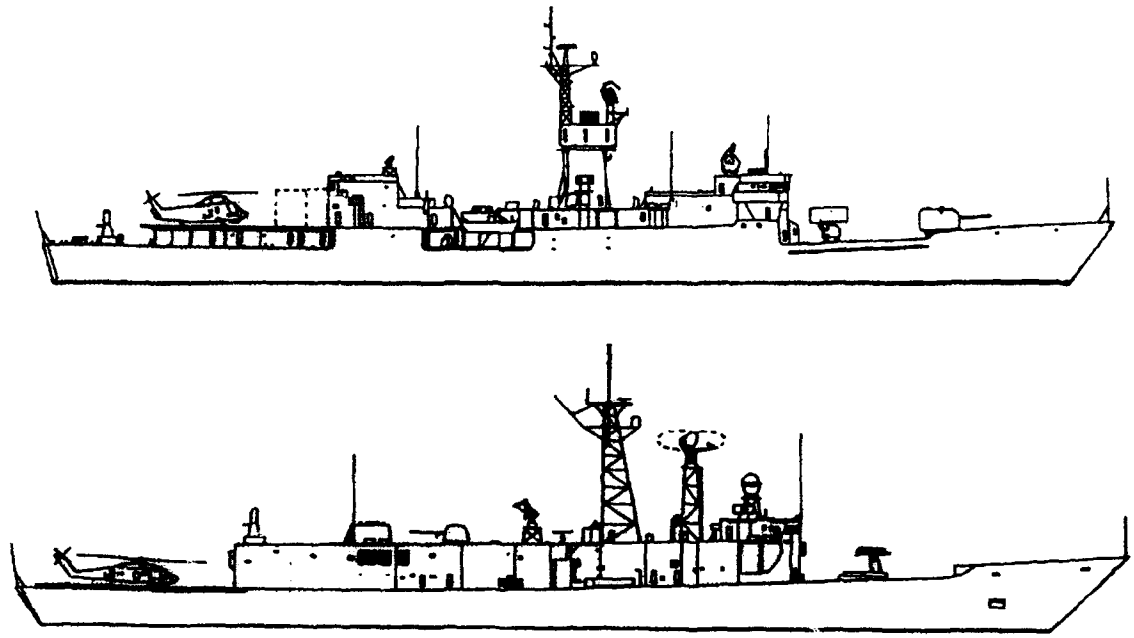

Fig. 4 Side views of FFG-7 'Oliver Hazard Perry' class frigate (bottom) and FF-1052 'Knox' class frigate (top)

values as a function of helicopter location and relative wind direction. The data do not correspond to uniform increments of helicopter location and the use of linear interpolation has its shortcomings.

It is not readily apparent how these profiles represent the flow field or how mean-flow and fluctuating velocities for a specified aircraft location can be determined from them. As a general observation, the profiles appear to be a somewhat simplified representation of velocities with a restrictive range of wind-over-deck directions (±30°). Since the operating envelope of the helicopter covers all angles of yaw, then this restriction limits the usefulness of the program.

For specified values of x_h', y_h', and z_h', dependent variables designated U_{xz}', U_{yz}', V_{xz}', F', W_{xz}', W_{yz}', u_{xz}', and u_{yz}' are obtained from the data base (Fig. 5) using linear interpolation. Using these dependent variables, non-dimensional velocities, designated U', V', W', and u', are determined for the chosen helicopter location by means of the following two relationships:

$$\begin{bmatrix} U' \\ V' \\ W' \end{bmatrix} = B \begin{bmatrix} U_{xz}' & U_{yz}' \\ V_{xz}' & F' \\ W_{xz}' & W_{yz}' \end{bmatrix} \tag{13}$$

$$u' = B\, u_{xz}'\, u_{yz}' \tag{14}$$

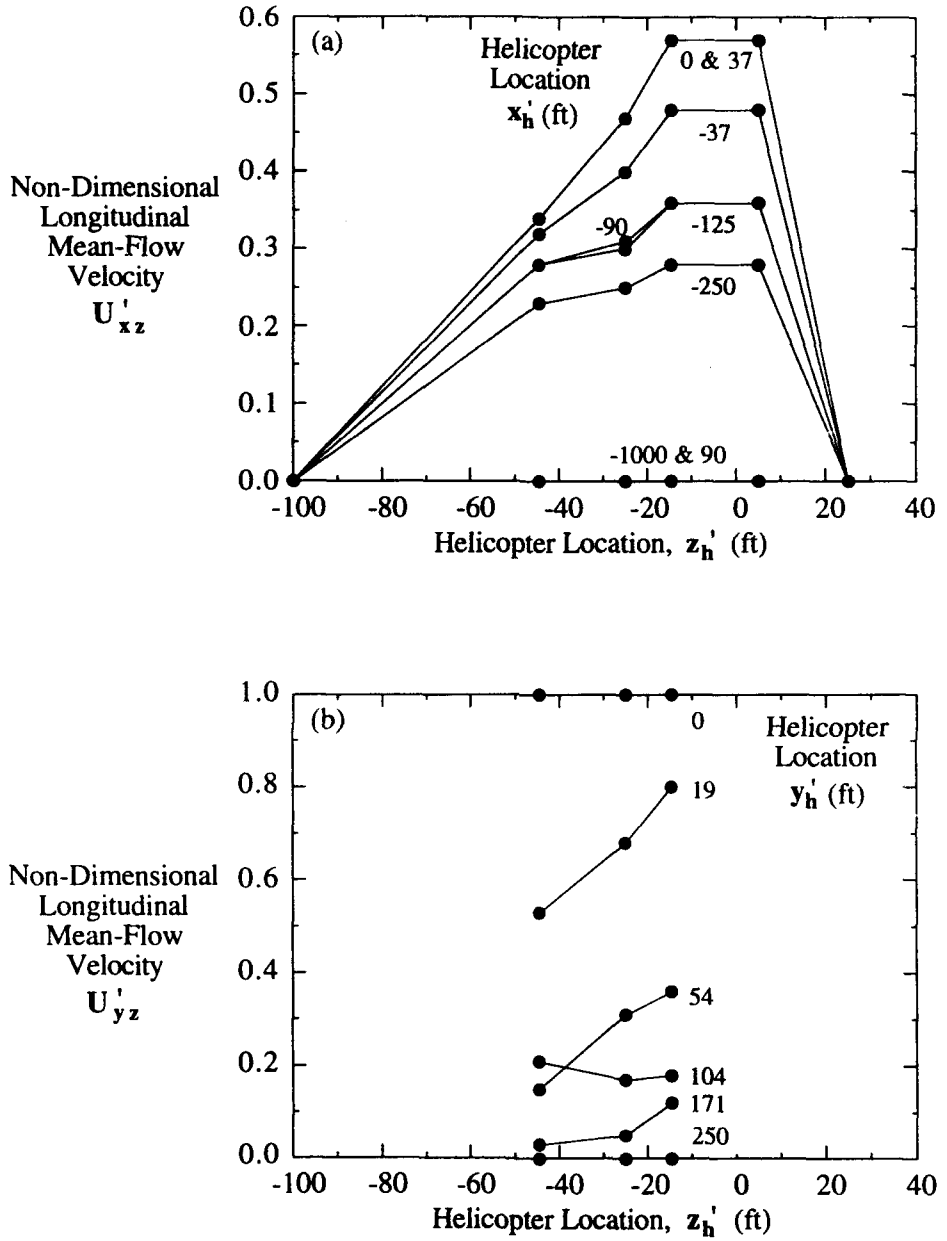

Fig. 5 Velocity profiles associated with the data base used in the simulation program; numbers near plotted lines refer to helicopter location

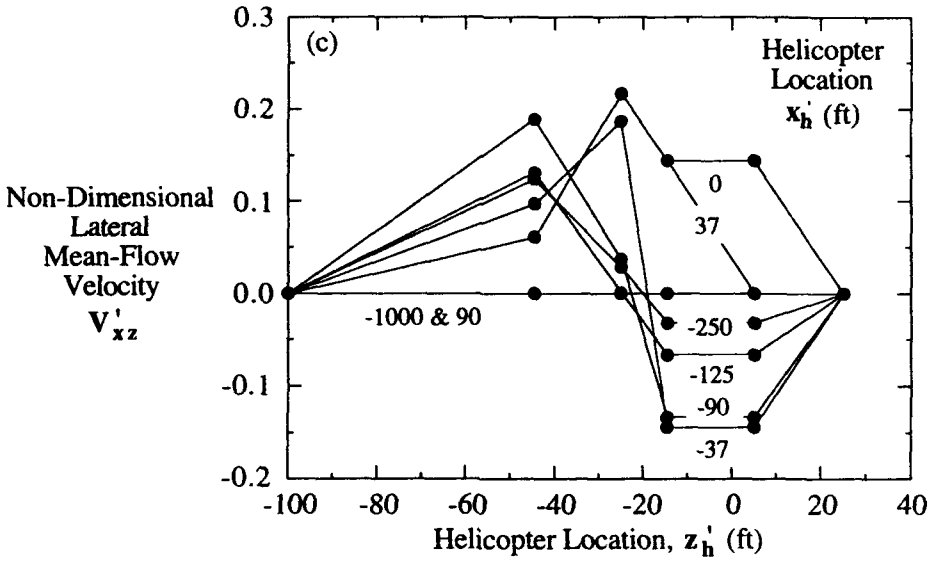

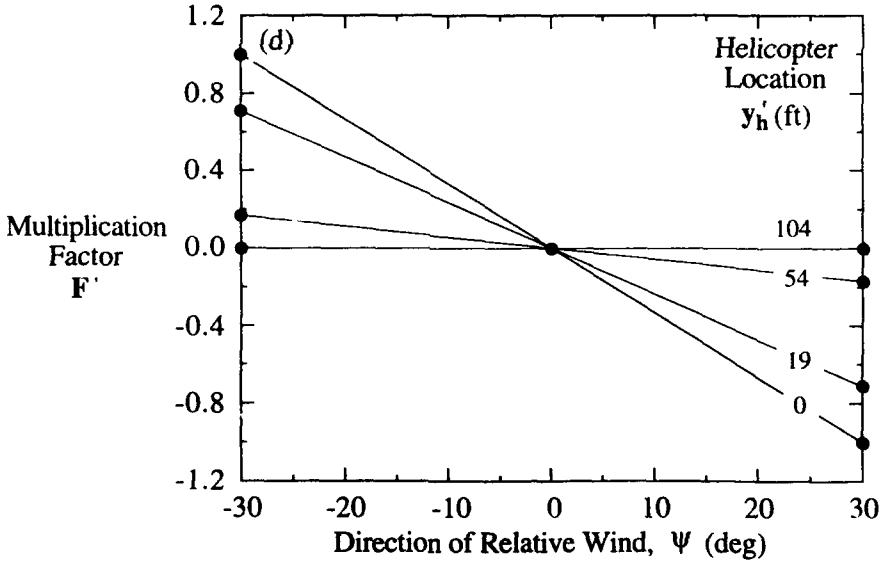

Fig. 5 (continued)

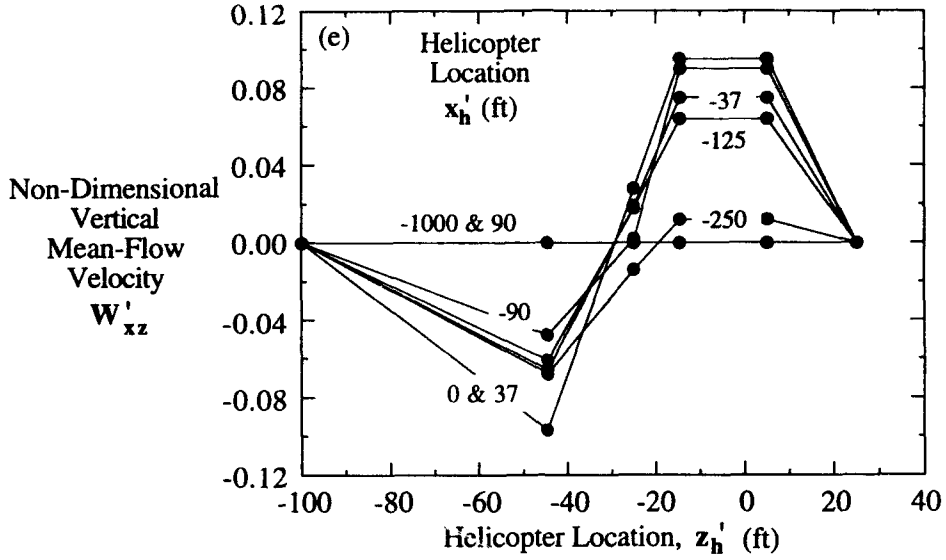

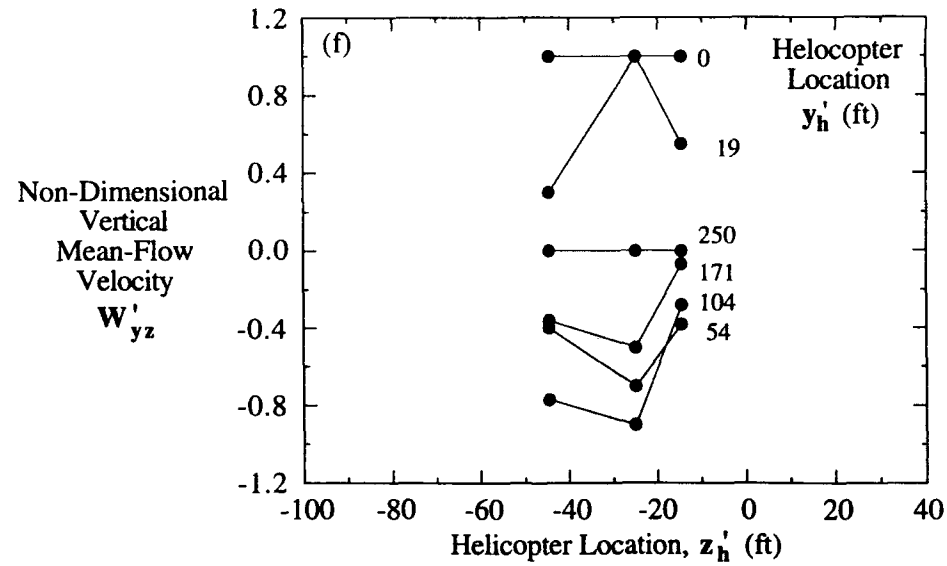

Fig. 5 (continued)

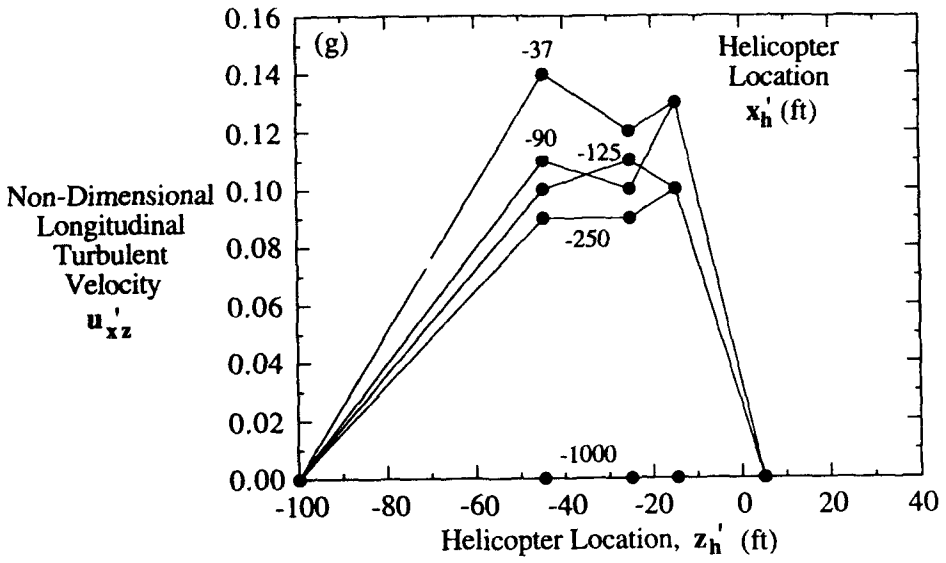

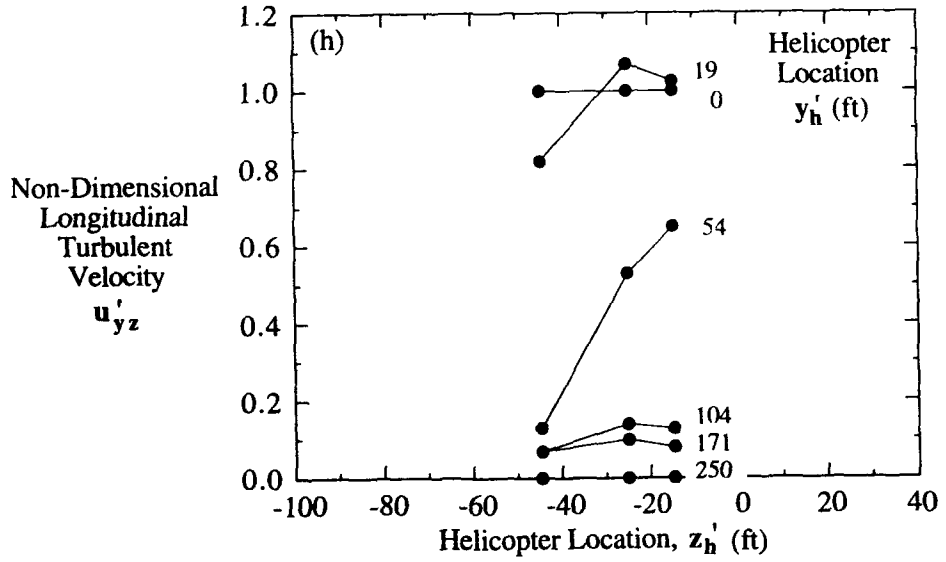

Fig. 5 (continued)

U ', V ', and W ' are mean-flow velocities in x'y'z' axes, and u' is a turbulent velocity in the x' direction. When calculating the variables, a washout factor, B, ramped in gradually, is used to reduce airwake effects if the pilot flies the helicopter forward of the origin of the x'y'z' axes or beyond 40° from the x' direction. The washout factor, which was in the supplied program, ensures that all ship-generated airwake velocities change gradually between the undisturbed free-stream and the airwake, with no abrupt interface.

Mean-flow velocities for the airwake, U_b, V_b, and W_b, are determined by resolving U ', V ', and W ' in xyz axes and dimensionalizing the terms, as shown below:

$$\begin{bmatrix} U_b \\ V_b \\ W_b \end{bmatrix} = U_{rel}[\lambda]_{sw} \begin{bmatrix} U' \\ V' \\ W' \end{bmatrix} \tag{15}$$

In this equation, U_{rel} is the velocity of the relative wind outside the airwake (see Fig. 3) and is used as a dimensionalizing factor. $[\lambda]_{sw}$ is the transformation matrix that is used to transform velocities from x'y'z' axes to xyz axes, and is given by

$$[\lambda]_{sw} = \begin{bmatrix} \cos\psi & -\sin\psi & 0 \\ \sin\psi & \cos\psi & 0 \\ 0 & 0 & 1 \end{bmatrix} \tag{16}$$

As with the atmospheric turbulence, fluctuations are incorporated into the turbulent velocities by the use of noise terms dependent on random numbers. For the airwake, these are given by the following relationship:

$$\begin{bmatrix} N_{bu} \\ N_{bv} \\ N_{bw} \end{bmatrix} = T_b \begin{bmatrix} |R_{11}| R_{11}\ \sigma_u \\ |R_{12}| R_{12}\ \sigma_v \\ |R_{13}| R_{13}\ \sigma_w H_{1F} \end{bmatrix} \tag{17}$$

N_{bu}, N_{bv}, and N_{bw} are analogous to N_{au}, N_{av}, and N_{aw} for subroutine ENVIR. T_b is the turbulence level for the airwake and has a default value of 3.0. N_{bu} and N_{bv} do not vary with altitude, whereas N_{bw} can vary with altitude via the height factor, H_{1F}, which is given by

$$H_{1F} = 0.1 \qquad \text{for } H > 100.0 \text{ ft} \tag{18a}$$

$$H_{1F} = 0.001\,H \qquad \text{for } H \leq 100.0 \text{ ft} \tag{18b}$$

As with atmospheric turbulence, it was found that the vertical turbulent velocities for the airwake, w_b, were far too small when compared with data measured on an FFG-7 (see Section 5). To obtain predicted and measured velocities of a comparable magnitude, H_{1F} was set to 1.0 for all heights.

The turbulence lag factor for the airwake, L_b, used when computing turbulent velocities, is given by

$$L_b = 1.0 - 0.01\, U_{tot}\, \Delta t_b \tag{19}$$

U_{tot} has been defined previously and Δt_b is the frame time for subroutine BURBLE which has a value of 0.0667 second, i.e. the airwake model operates at 15 Hz, in phase with the atmospheric model.

Although the airwake model used in the simulation program and that used by Fortenbaugh (Refs 3, 7, and 8) both use the same wind tunnel data of Garnett, documented in Ref. 4, there are some notable differences between the two airwake models. In particular, the methods used to determine turbulent velocities in the two cases are different. Fortenbaugh determines turbulent velocities by using a general differential equation, whereas the simulation program uses a simple autoregression as shown in Equation 12. Also, Fortenbaugh determines airwake velocities by simply adding mean-flow and turbulent components, whereas the simulation code uses weighting as shown in Equation 11.

3.3 Subroutine WINDC

Subroutine WINDC simply calls ENVIR and BURBLE and adds the simulation velocities computed by these two subroutines (such as u_a and U_b^*)

4. PREDICTED VELOCITIES

The simulation program determines the total simulation velocities for the three ship-coordinate directions by adding individual components of velocity, viz mean-flow free-stream velocities, velocities due to atmospheric turbulence, and incremental airwake velocities, as follows:

$$\begin{bmatrix} U \\ V \\ W \end{bmatrix} = \begin{bmatrix} U_a \\ V_a \\ W_a \end{bmatrix} + \begin{bmatrix} u_a \\ v_a \\ w_a \end{bmatrix} + \begin{bmatrix} U_b^* \\ V_b^* \\ W_b^* \end{bmatrix} \tag{20}$$

Velocities predicted for the FFG-7 using the program will now be examined. This will be done for some sample helicopter/ship operating conditions which have been chosen to be a 35 knot relative wind 30° off the starboard bow and for a height of 21.0 ft above the bullseye. This height corresponds to the mid location of the Gill anemometers used for velocity measurements on HMAS Darwin, which is an FFG-7 (see Section 5).

The free-stream velocities, U_a, V_a, and W_a, due to the constant 35 knot relative wind, have values of –51.2, –29.6, and 0 ft/s respectively. Fig. 6 shows background atmospheric turbulence velocity for H_F = 1.0 (Fig. 6a), incremental airwake velocity for H_{1F} = 1.0 (Fig. 6b), and total simulation velocity (Fig. 6c), each for three coordinate directions. The velocities in these plots were computed at time intervals of 0.0667 second.

The vertical turbulent velocities in the supplied code may have been set very low since an actuator disk type of rotor model is used in the code. For such a rotor model, it is assumed that calculated velocities act uniformly over the entire rotor. It may therefore have been necessary to reduce vertical velocities to avoid excessive loading of the rotor resulting from this unrealistic situation. It will be desirable in the future to modify the program to take account of velocity variations over the helicopter.

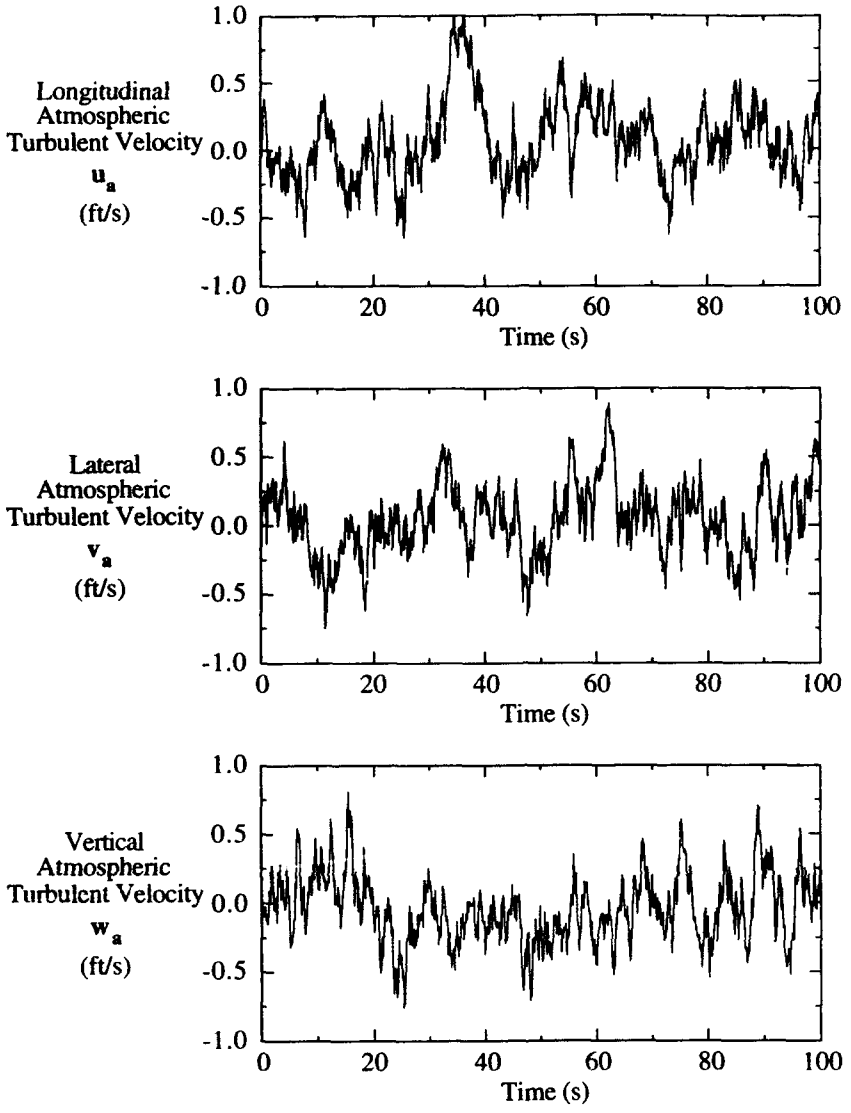

Fig. 6a Velocities due to background atmospheric turbulence for a 35 knot relative wind 30° off the starboard bow and for 21.0 ft above bullseye

It is important to note that the total simulation velocities, U, V, and W, are only calculated for the centre of gravity of the helicopter and it is assumed that these velocities are constant over the entire space occupied by the helicopter. Since the dimensions of the helicopter rotor are comparable with the beam of the ship and the lateral size of the wake, then such a simplification is a limitation of the simulation procedure. No account is taken of the effects on helicopter behaviour of non-uniform velocity distributions over the rotor blades. The accuracy and validity of such a simplified method is questionable since the helicopter behaviour during the hazardous approach and landing phase is intimately connected with the incident flow on its blades. Coupled with this, the simulation program currently uses an actuator disk type of rotor model. Such a model does not provide a fully credible representation of flight in turbulent airwakes. Rapid angle of attack changes on the rotor blades induced by turbulence and mean-flow velocity gradients are ignored. As part of the development of the simulation program, it is

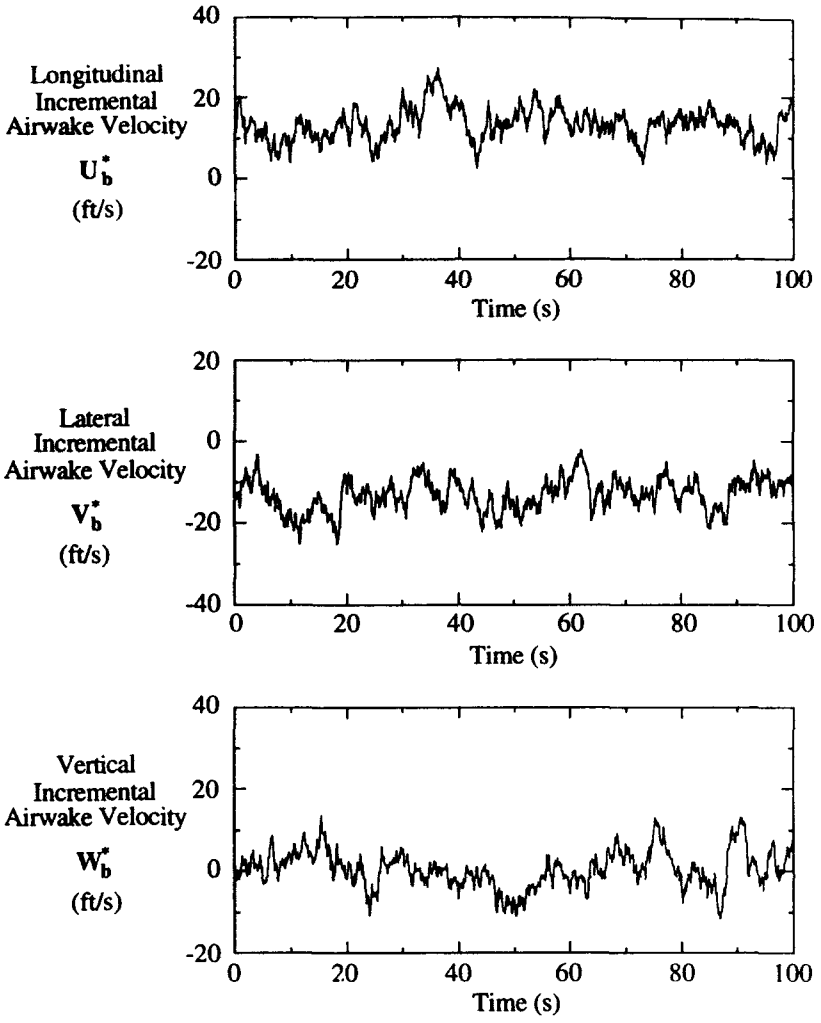

Fig. 6b Incremental airwake velocities for conditions given in Fig. 6a

anticipated that a blade element type of rotor model will be incorporated into the program to replace the actuator disk model currently used so that variation in velocities over the helicopter main rotor can be considered more realistically.

To determine the dominant energy-containing frequencies of fluctuating velocities, it is necessary to do a spectral analysis. Fig. 7 shows spectra for three coordinate directions corresponding to the total simulation velocities shown in Fig. 6c. The spectra were obtained from the velocity plots by using a Fast-Fourier-Transform (FFT) algorithm, where the number of data points required for the algorithm is a power of two. The velocities shown in Fig. 6c were computed at every 0.0667 second for 100 seconds, which means that each velocity plot shown corresponds to about 1500 data points. Therefore 1024 (= 2^{10}) points were used in the spectral analysis, which is equivalent to 68.2 seconds of a velocity plot. The frequencies shown in Fig. 7 range from 0.0146 Hz to 7.4854 Hz in increments of 0.0146 Hz, i.e. 1/(0.0667 x 1024) Hz. The spectra shown in Fig. 7 have not been smoothed in any way.

Whenever a finite number of points is chosen to represent fluctuating velocity waveforms, then the mean velocities near the beginning and end of the finite sample can be significantly different. When computing spectra from these waveforms, such behaviour can be interpreted as a low-frequency phenomenon coupled with high frequency effects due to the step change

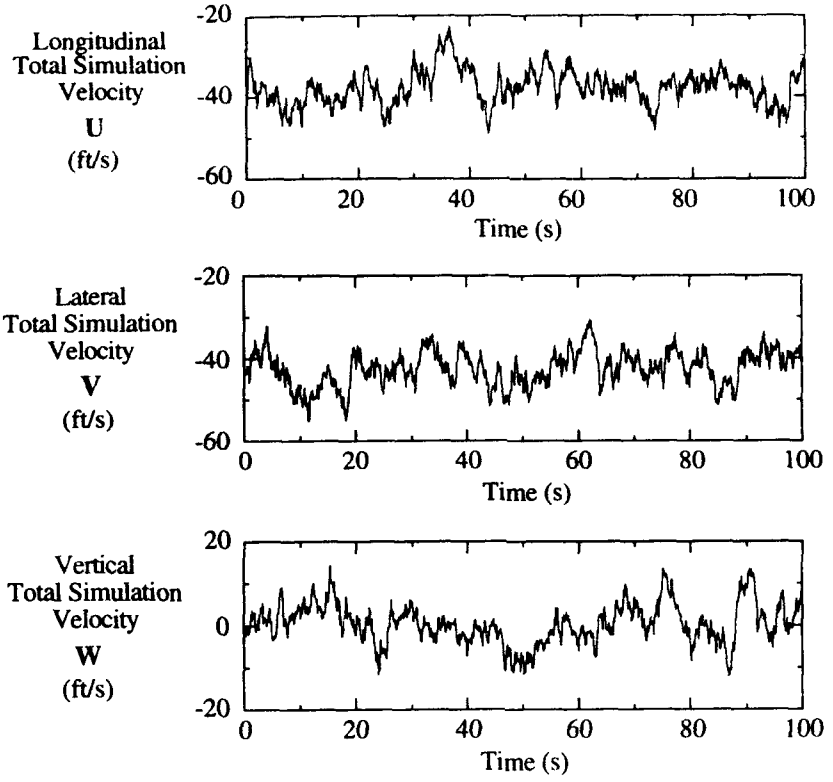

Fig. 6c Total simulation velocities for conditions given in Fig. 6a

between the beginning and end of the sample, and can cause an increase in spectral densities at low-frequencies. There are ways of correcting for this and one such method is to apply a Blackman window to the data – see Ref. 15. A Blackman window adjusts velocities so that their values at the start and finish of the chosen range are gradually diminished, becoming zero at the extremes. The application of a Blackman window also smooths spectra. This is done by first smoothing with a Hanning window and then further smoothing with weights of 0.16, 0.68, and 0.16 (see Ref. 15 for details). Spectra corresponding to those shown in Fig. 7 were computed using this method and the smoothed spectra are shown in Fig. 8. It can be seen that the main effect of the Blackman window is to smooth the spectra by reducing the amplitude of the spikes.

The effect on spectra of choosing consecutive sets of 1024 data points is shown in Fig. 9 for longitudinal total simulation velocities. There is good agreement for the two spectra, which was also the case for the other two components of velocity.

Spectra are often plotted in premultiplied form, whereby power spectral densities are multiplied by their associated frequencies and the product of these two terms is plotted against logarithm of frequency. Spectra shown in Fig. 8 were recomputed in premultiplied form and the resulting spectrum for longitudinal velocities is shown in Fig. 10. Such a plot indicates the energy contribution over any frequency range as an area under the curve. It is apparent that most of the energy of the fluctuating velocity is associated with frequencies below about 1.0 Hz, i.e. the most energetic eddies are of a comparable size to the beam of the ship. Similar behaviour occurred for the spectra for the other two components of velocity.

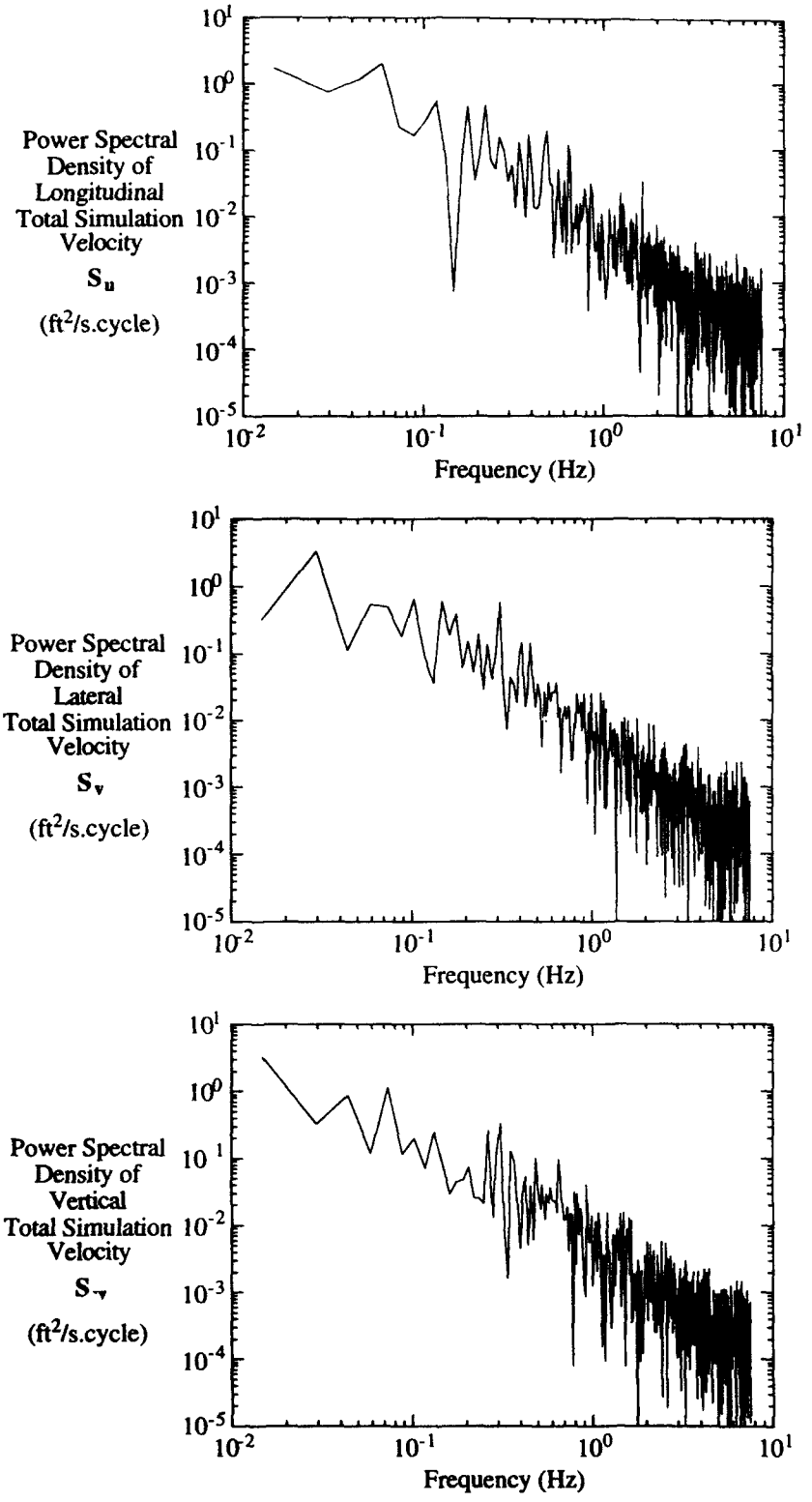

Fig. 7 Spectra corresponding to total simulation velocities shown in Fig. 6c

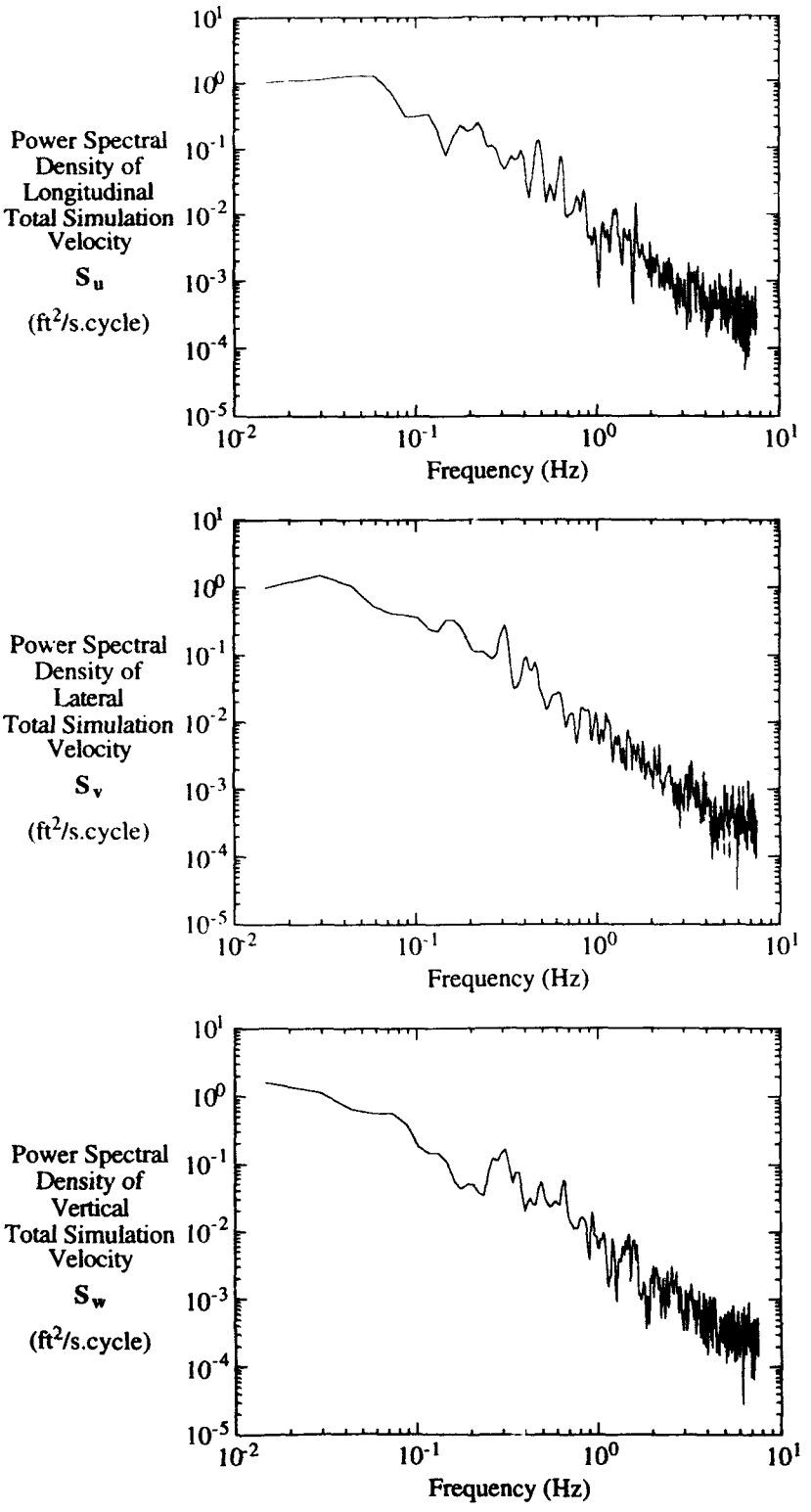

Fig. 8 Spectra corresponding to total simulation velocities shown in Fig. 6c; spectra have been processed using a Blackman window

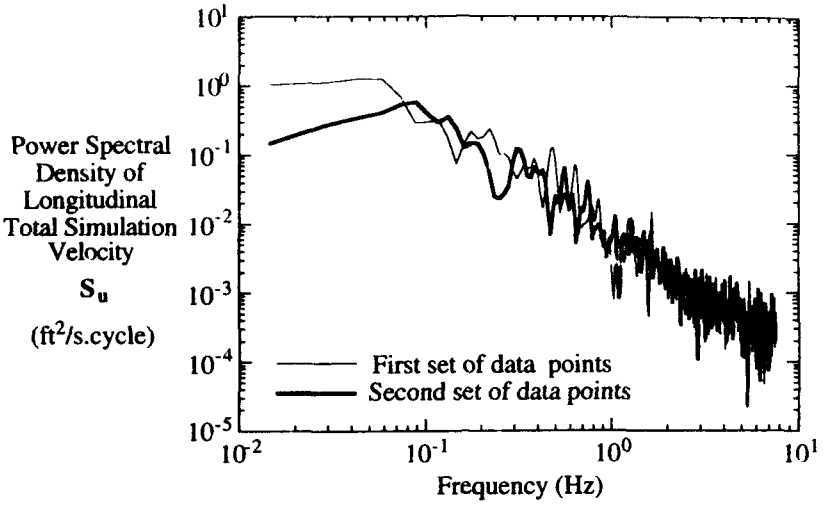

Fig. 9 Effect of choosing different samples in calculating spectra corresponding to longitudinal total simulation velocities shown in Fig. 6c; spectra have been processed using a Blackman window

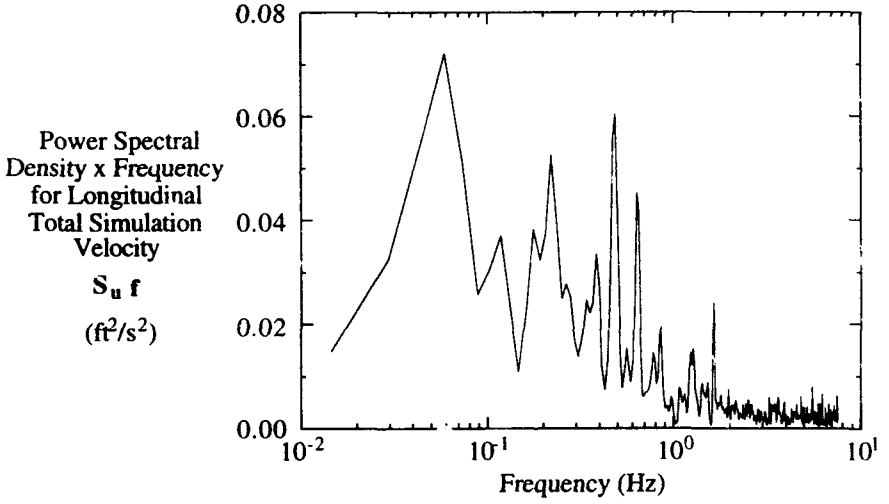

Fig. 10 Premultiplied spectra corresponding to longitudinal total simulation velocities shown in Fig. 6c

A spectrum for the atmospheric turbulent velocity, u_a, is shown in Fig. 11. According to von Karman, atmospheric spectra are expected to follow a line of slope -5/3 at high frequencies when plotted on log-log coordinates (see Ref. 13). This behaviour is seen in Fig. 11 for u_a and also occurs for v_a and w_a, indicating that the airwake model produces spectra having realistic slopes at high frequencies.

5. COMPARISON BETWEEN PREDICTED AND MEASURED VELOCITIES

Velocities were measured at three different heights above the bullseye on HMAS Darwin using Gill anemometers (see Refs 16 to 18) and the measurements were taken in the absence of a helicopter. The heights of the anemometers were 10.5 ft, 21.0 ft, and 31.5 ft. The

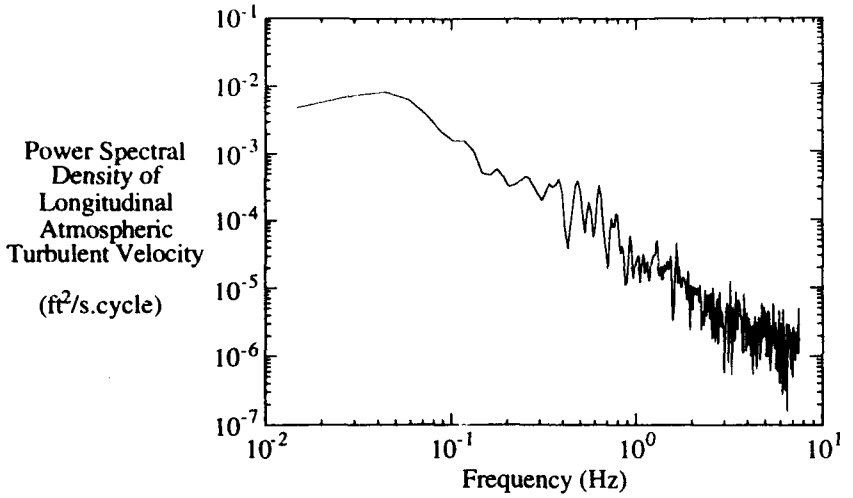

Fig. 11 Spectrum corresponding to longitudinal atmospheric turbulent velocities shown in Fig. 6a

comparison between predicted and measured velocities will be made for operating conditions consisting of a 35 knot relative wind at 30° off the starboard bow and for the above three heights. This combination of wind speed and direction was chosen since in this case the effects of ship motion on the measured velocities was small. Also, the 30° case is typically used by researchers in the field, e.g. Ref 19. Conditions were set precisely in the simulation code when predicting velocities, but for the measurements, some variations in the magnitude and direction of the relative wind occurred naturally.

Predicted and measured velocities are shown superimposed in Fig. 12 for the longitudinal, lateral, and vertical directions. The thin lines correspond to predicted velocities and the thick lines to measured velocities. The measurements have not been corrected for the effects of ship motion.

For the velocities shown in Fig. 12 it is not intended to compare fluctuating components since this should be done using spectral analysis. However, the mean values of corresponding velocities in the longitudinal and lateral directions are markedly different in most cases. Mean values of corresponding velocities in the vertical direction show reasonable agreement in all cases.

Predicted and measured velocities for a 35 knot relative wind at 30° off the starboard bow are further compared in Fig. 13, which depicts mean velocities in a horizontal plane for a height of 21.0 ft above the flight deck. As can be seen, there are some large differences between predicted and measured velocities, both in terms of magnitude and direction. The large differences that often occur between predicted and measured mean velocities in the above comparisons suggest that the model used for prediction should be based on measurements for an FFG-7, and not on measurements for an FF-1052, as it is presently. Further measurements on an FFG-7, either in a wind tunnel or on a full-scale ship, are needed to develop a better description of the flow. No other information from the US has been provided as validation of the code. Also, the data in the data base do not correspond to uniform increments of helicopter location and the use of linear interpolation to determine velocities has its shortcomings.

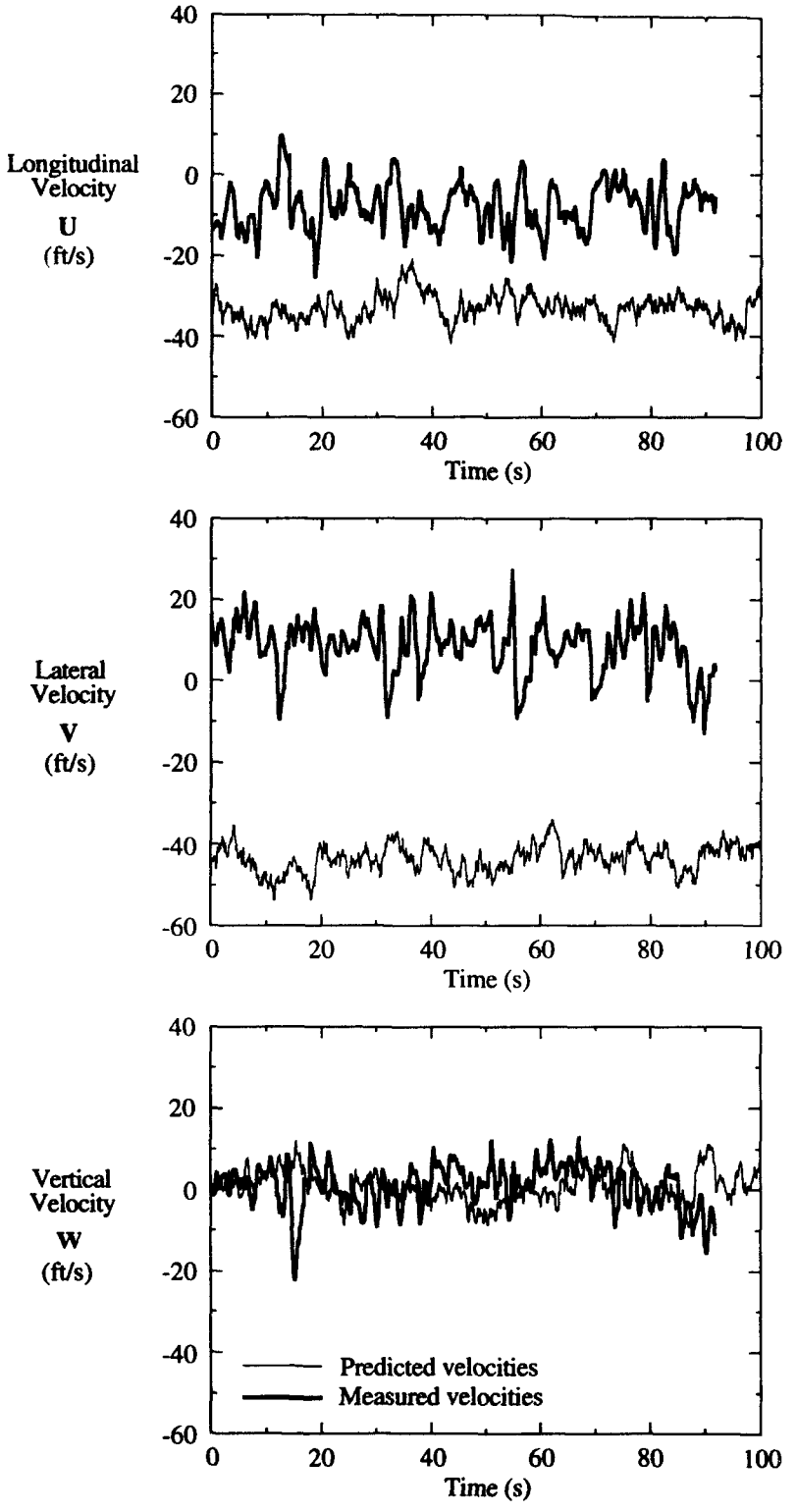

Fig. 12a Comparison between predicted and measured velocities for a 35 knot relative wind at 30° off starboard bow and for 10.5 ft above bullseye

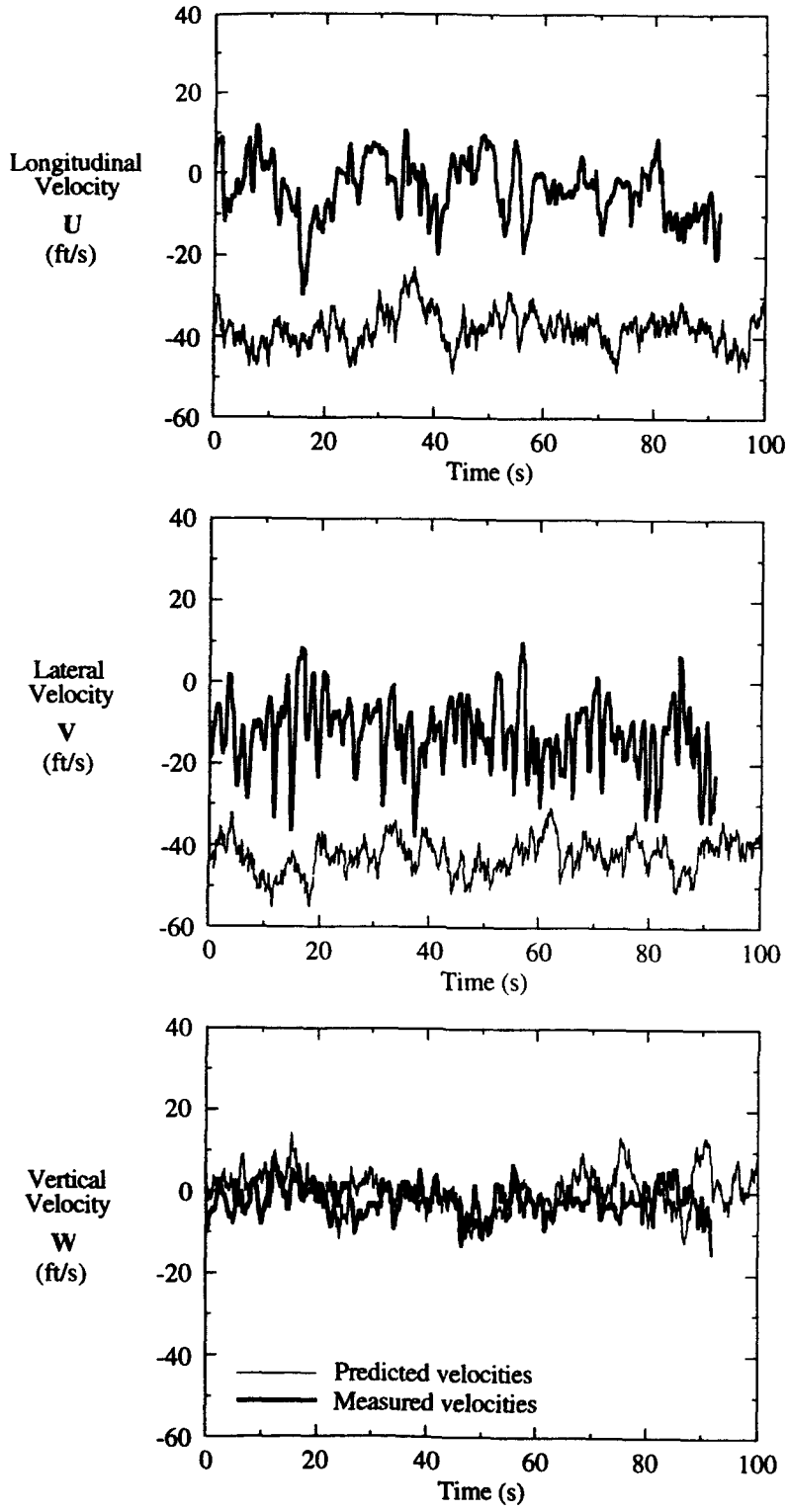

Fig. 12b Comparison between predicted and measured velocities for a 35 knot relative wind at 30° off starboard bow and for 21.0 ft above bullseye

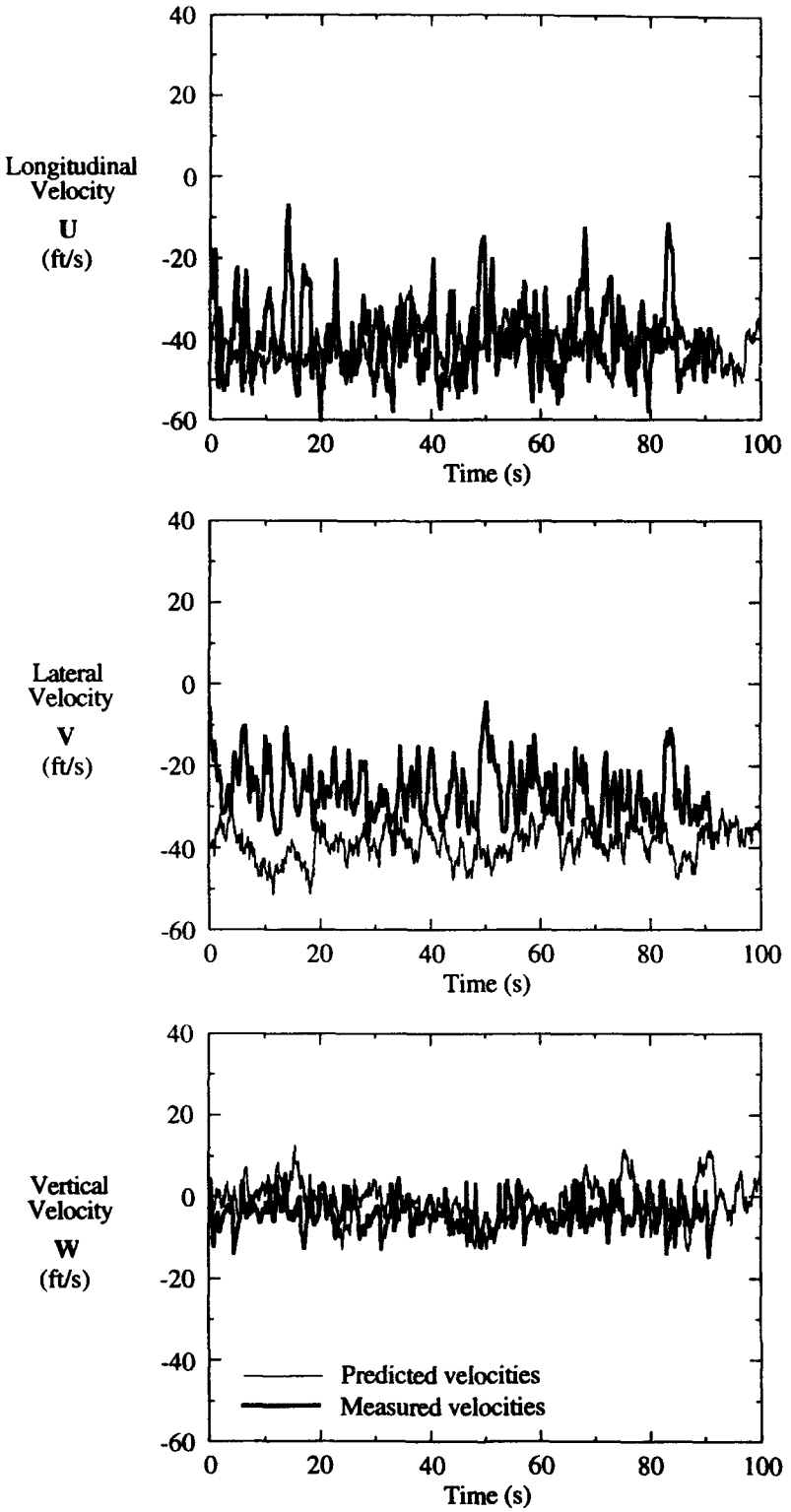

Fig. 12c Comparison between predicted and measured velocities for a 35 knot relative wind at 30° off starboard bow and for 31.5 ft above bullseye

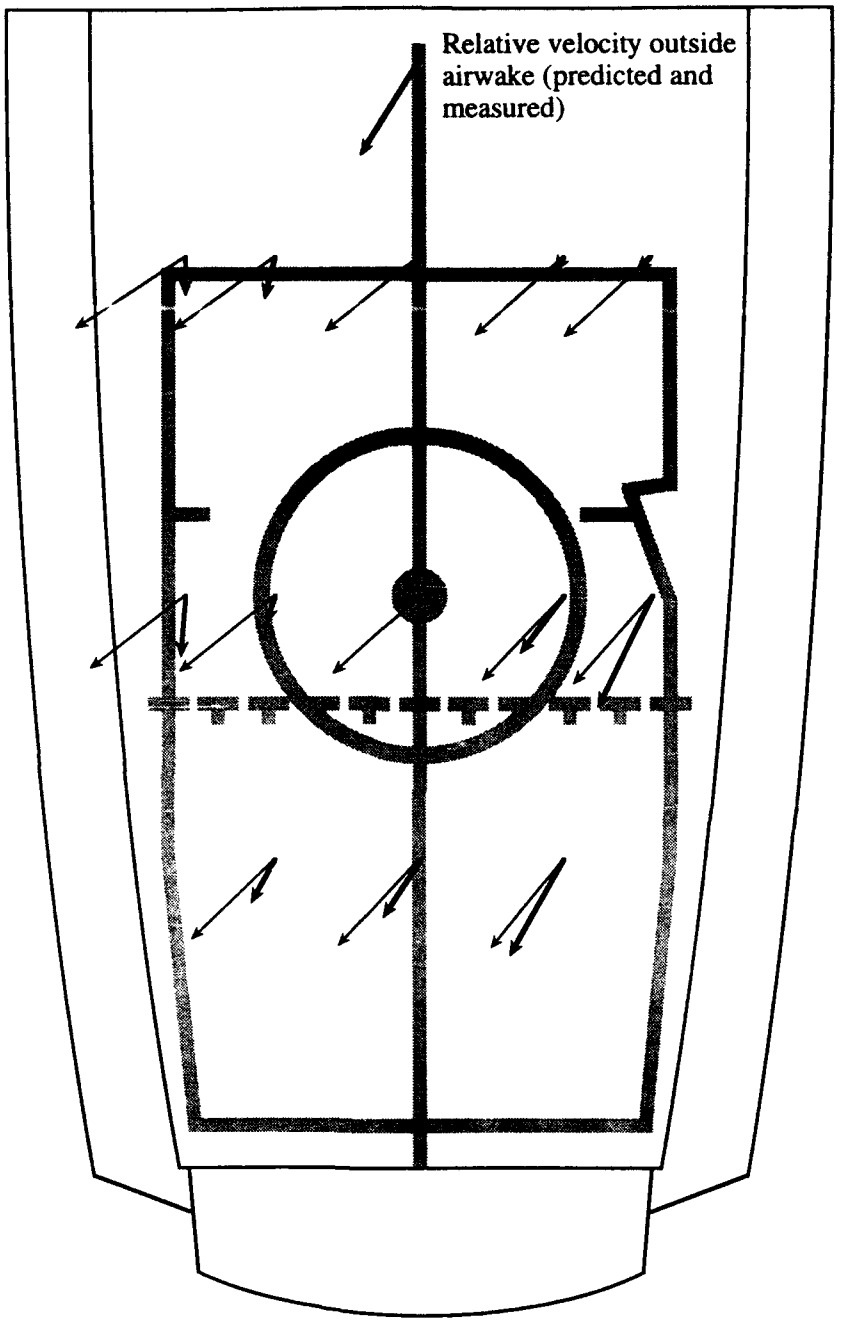

Fig. 13 Comparison between predicted and measured velocities for a 35 knot relative wind at 30° off starboard bow and for 21.0 ft above bullseye
——— predicted velocities; ——— measured velocities

Spectra corresponding to the velocities shown in Fig. 12b (which corresponds to 21.0 ft above the bullseye) are shown superimposed in Fig. 14. The spectra for measured velocities are based upon 1024 consecutive points, as for spectra for predicted velocities, but since the measured velocities were determined at intervals of 0.05 second, and not 0.0667 second as for the predicted velocities, then the spectra for measured velocities correspond to 51.2 seconds of a velocity plot and the frequency range covered varies from 0.0195 Hz to 9.9805 Hz in increments of 0.0195 Hz. The reason for the difference in time intervals is that the simulation code and the data acquisition equipment used on HMAS Darwin were developed independently. The spectra shown accurately represent the measured velocity signals. It is realised, however, that the anemometers have a maximum frequency response of about 2.5 Hz, and thus the measurements do not accurately represent the actual true velocities, especially at the higher frequencies. The agreement between spectra corresponding to predicted and measured velocities is generally good.

The airwake turbulence is caused by eddies separating from the ship, like a Karman vortex street, and the instant of separation of vortices will be greatly influenced by the rolling and pitching of the ship. This will affect the frequency spectrum: it may or may not have much effect on turbulence intensities, but it is an extra difficulty of using a still model in a wind tunnel to simulate a pitching and rolling ship on the sea.

6. CONCLUSIONS

The investigation is concerned with studying the airwake model in the SH-60B/FFG-7 simulation program and analysing the resultant airwake over the flight deck of an FFG-7 class frigate. Comparisons were made between velocities predicted by the program and those measured during full-scale tests on HMAS Darwin. Marked differences between observed and calculated mean-flow velocities were found to occur for the operating conditions chosen.

A likely contributing factor to the lack of agreement is that the data within the data base in the simulation program are based upon wind-tunnel measurements using a model of an FF-1052 class frigate, which has a markedly different superstructure. The data in the data base are somewhat sparse and are only given for wind-over-deck directions varying within the range $\pm 30^{\circ}$ from the ship centreline. This restriction limits the usefulness of the program.

The simulation program only calculates velocities at the centre of gravity of the helicopter and it is assumed that these velocities exist over all regions of the helicopter. No account is taken of the effects on helicopter behaviour of non-uniform velocity distributions over the rotor blades. The accuracy and validity of such a simplified approach is questionable since the helicopter behaviour during the hazardous approach and landing phase is intimately connected with the incident flow on its blades. It is desirable now to modify the program to take account of velocity variations over the helicopter. Coupled with this, the simulation program currently uses an actuator disk type of rotor model. Such a model does not provide a fully credible representation of flight in turbulent airwakes. Rapid angle of attack changes on the rotor blades induced by turbulence and mean-flow velocity gradients are ignored. For future airwake models to be effective, they will have to be implemented in conjunction with a blade-element type of rotor model that senses velocity gradients across the rotor.

ACKNOWLEDGEMENTS

The author is indebted to Dr N. E. Gilbert, Mr A. M. Arney, and Dr N. Matheson for their help during the course of this work, and to Mr B. D. Forrester and Dr D. J. Sherman for their advice on spectral analysis.

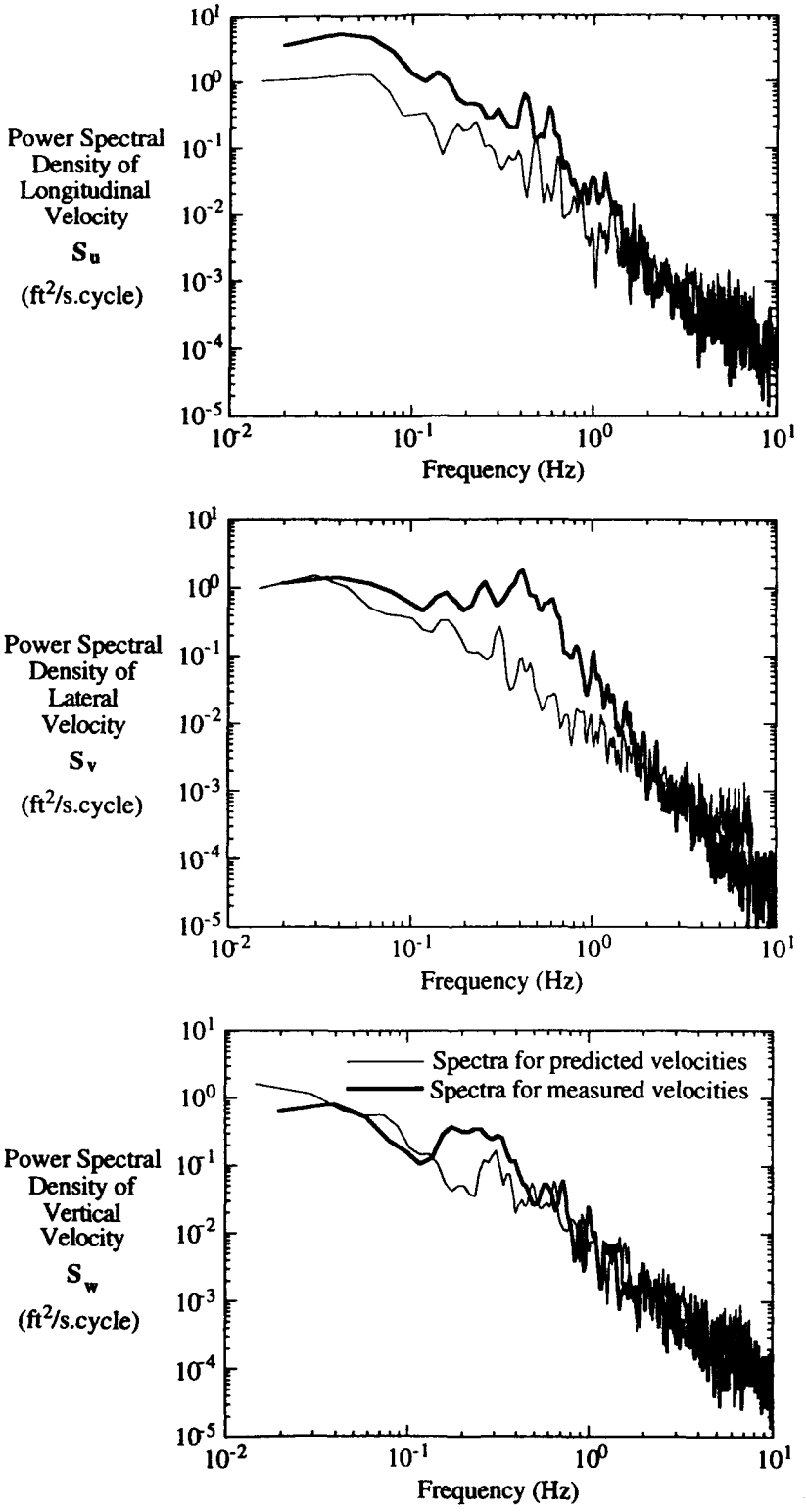

Fig. 14 Comparison between spectra corresponding to predicted and measured velocities shown in Figure 12b

REFERENCES

1. Arney, A. M., Blackwell, J. & Feik, R. A. "Modelling the Helicopter/Ship Dynamic Interface," *Australian Aeronautical Conference*, Institution of Engineers, Australia, Melbourne, 9-11 October, 1989.
2. Blackwell, J. & Feik, R. A. "A Mathematical Model of the On-Deck Helicopter/Ship Dynamic Interface," *ARL Tech Memo 405,* Aero Res Lab, Melbourne, September 1988.
3. Fortenbaugh, R. L. " A Math Model for the Airwake of a DE 1052 Class Ship," *Report 2-53300/7R-3397*, Vought Corporation, Dallas, Texas, US, May 1977.
4. Garnett, T. S. Jr. "Investigation to Study the Aerodynamic Ship Wake Turbulence Generated by an FF1052 Frigate," *Boeing-Vertol Report D210-11140-1*, Philadelphia, Pennsylvania, US, December 1976.
5. Healey, J. V. "The Prospects for Simulating the Helicopter/Ship Interface," *Naval Engineers Journal*, Vol 99, pp. 45-63, March 1987.
6. Healey, J. V. "Simulating the Helicopter-Ship Interface as an Alternative to Current Methods of Determining the Safe Operating Envelopes," *NPS67-86-003,* Naval Postgraduate School, Monterey, California, US, September 1986.
7. Fortenbaugh, R. L. "Mathematical Models for the Aircraft Operational Environment of DD-963 Class Ships," *Report 2-55800/8R-3500*, Vought Corporation, Dallas, Texas, US, September 1978.
8. Fortenbaugh, R. L. "Progress in Mathematical Modelling of the Aircraft Operational Environment of DD 963 Class Ships," *AAIA Paper No. 79-1677,* Atmospheric Flight Mechanics Conference, Boulder, Colorado, US, August 1979.
9. Nave, R. L. "Development and Analysis of a CVA and a 1052 Class Fast Frigate Air Wake Model," *NADC Report 78182-60*, Philadelphia, Pennsylvania, US, September 1978.
10. Garnett, T. S. Jr. "Investigation to Study the Aerodynamic Ship Wake Turbulence Generated by an DD963 Destroyer," *Boeing-Vertol Report D210-11545-1*, Philadelphia, Pennsylvania, US, August 1979.
11. Hanson, G. D. "Airwake Analysis," *Working Paper No. 1198-3,* Systems Technology Incorporated, California, US, September 1983.
12. Roll, H. U. "Physics of the Marine Atmosphere," Academic Press, London, UK, 1965.
13. "Characteristics of Atmospheric Turbulence Near the Ground, Part II: Single Point Data for Strong Winds (Neutral Atmosphere)," *ESDU Item Number 85020* (Supersedes Item Number 74031), Engineering Sciences Data Unit, 251–259 Regent Street, London, W1R 7AD, UK, 1985.
14. Box, G. E. P. & Jenkins, G. M. "Time Series Analysis Forecasting and Control," Holden-Day, San Francisco, US, 1970.
15. Blackman, R. B. "Linear Data-Smoothing and Prediction in Theory and Practice," Addison-Wesley, Massachusetts, US, 1965.
16. Sutton, C. W. "FFG-7 Extended Deck Ship Motion and Airwake Sea Trial (Trials Instruction for ARL Trial 1/89)," *ARL Flight Mech Tech Memo 414,* Aero Res Lab, Melbourne, June 1989.

17. Arney, A. M. "Preliminary Report on the FFG-7 Extended Deck Ship Motion and Airwake Sea Trial: Part I - Instrumentation Calibration Data," *Group Report 90/3 (unpublished)*, Aero Res Lab, Melbourne, May 1990.

18. Arney, A. M. "Preliminary Report on the FFG-7 Extended Deck Ship Motion and Airwake Sea Trial: Part II - Data Processing Procedures," *Group Report 90/4 (unpublished)*, Aero Res Lab, Melbourne, July 1990.

19. Healey, J. V. "Establishing a data base for flight in the wakes of structures," *Journal of Aircraft*, **29**, No 4, 559-564, Jul-Aug 1992.

APPENDIX A

FORTRAN VARIABLES IN AIRWAKE MODULE

Fortran Variable	Symbol	Description of Variable (As Given in SH-60B Simulation Program)	Dimension
AFGALT	G_l	Turbulence altitude gain	
AFHGR	H	Altitude of helicopter main gear above sea level	ft
AFLAGF	L_a	Turbulence lag factor for atmosphere	
AFPSIW	Ψ_{amb}	Wind direction - Chosen initial condition	deg
AFRN	R_{11}, R_{12}, R_{13}	Random numbers -1.0 to +1.0	
AFTEMP	H_F	Description of variable not given in program	
AFTGAIN	G	Turbulence gain factor	
AFTL	T_a	Turbulence level - Chosen initial condition	
AFUSIG	σ_u	x-axis standard deviation turbulent velocity	ft/s
AFUTRB	u_a	x- axis turbulence velocity	ft/s
AFVP	U_{tot}	Velocity of the relative wind	ft/s
AFVSIG	σ_v	y-axis standard deviation turbulent velocity	ft/s
AFVTRB	v_a	y- axis turbulence velocity	ft/s
AFVW	U_{amb}	Wind velocity - Chosen initial condition	ft/s
AFVWD		Total horizontal wind velocity	ft/s
AFWDR		Wind direction	rad
AFWN1	N_{au}	x-axis scaled white noise	
AFWN2	N_{av}	y-axis scaled white noise	
AFWN3	N_{aw}	z-axis scaled white noise	
AFWSIG	σ_w	z-axis standard deviation turbulent velocity	ft/s
AFWTRB	w_a	z- axis turbulence velocity	ft/s
ARBWO	B	Burble washout total	
ARDTWOD		Turbulence adjustment increment	
ARDXWOD		x-axis adjustment increment	
ARDYWOD		y-axis adjustment increment	
ARDZWOD		z-axis adjustment increment	

APPENDIX A Cont'd

FORTRAN VARIABLES IN AIRWAKE MODULE

Fortran Variable	Symbol	Description of Variable (As Given in SH-60B Simulation Program)	Dimension
ARKTLU		Turbulence burble gain x-axis	
ARKTLV		Turbulence burble gain y-axis	
ARKTLW		Turbulence burble gain z-axis	
ARKTLY	u'_{yz}	Turbulence, y-z plane	
ARKTWOD		Turbulence gain	
ARKVXY	U'_{yz}	x-axis burble, y-z plane	
ARKVYY	F'	y-axis burble, wind-over-deck and y distance	
ARKVZY	W'_{yz}	z-axis burble, y-z plane	
ARKXL	F	Total burble effects factor	
ARKXWOD		x-axis burble gain	
ARKYWOD		y-axis burble gain	
ARKZWOD		z-axis burble gain	
ARLAGF	L_b	Turbulence lag factor for burble	
ARPSI		Ship heading	deg
ARTL	T_b	Ship burble turbulence level	
ARTL1	u'_b	Turbulence increment	ft/s
ARTLB	u'	Burble turbulence	
ARTLXZ	u'_{xz}	Turbulence, x-z plane	
ARUS1	U_b	x burble increment, steady state	ft/s
ARUSWND	U^*_b	x-velocity increment, burble	ft/s
ARUTL	u_b	x burble increment, dynamic	ft/s
ARVS1	V_b	y burble increment, steady state	ft/s
ARVSWND	V^*_b	y-velocity increment, burble	ft/s
ARVTL	v_b	y burble increment, dynamic	ft/s
ARVXB	U'	x burble wind velocity	
ARVXXZ	U'_{xz}	x-axis burble, x-z plane	

APPENDIX A Cont'd

FORTRAN VARIABLES IN AIRWAKE MODULE

Fortran Variable	Symbol	Description of Variable (As Given in SH-60B Simulation Program)	Dimension
ARVYB	V'	y burble wind velocity	
ARVYXZ	V'_{xz}	y-axis burble, x-z plane	
ARVZB	W'	z burble wind velocity	
ARVZXZ	W'_{xz}	z-axis burble, x-z plane	
ARWN1	N_{bu}	x-axis scaled white noise	
ARWN2	N_{bv}	y-axis scaled white noise	
ARWN3	N_{bw}	z-axis scaled white noise	
ARWOD	U_{rel}	Wind-over-deck velocity	ft/s
ARWODD	ψ	Wind-over-deck direction	deg
ARWS1	W_b	z burble increment, steady state	ft/s
ARWSWND	W_b^*	z-velocity increment, burble	ft/s
ARWTL	w_b	z burble increment, dynamic	ft/s
ARXBIV	x_h'	x-axis burble variable	ft
ARYBIV	y_h'	y-axis burble variable	ft
ARZBIV	z_h'	z-axis burble variable	ft
AZRAND1	R_{21}	Random number 0.0 to +1.0	
AZRAND2	R_{22}	Random number 0.0 to +1.0	
AZRAND3	R_{23}	Random number 0.0 to +1.0	
DTBURB	Δt_b	Frame time for Subroutine BURBLE	s
DTENVIR	Δt_a	Frame time for Subroutine ENVIR	s
VDW	W_a	Downward component of wind	ft/s
VEW	V_a	Eastward component of wind	ft/s
VNW	U_a	Northward component of wind	ft/s
VTWD	W	Downward wind component including turbulence	ft/s
VTWE	V	Eastward wind component including turbulence	ft/s
VTWN	U	Northward wind component including turbulence	ft/s

APPENDIX B

FORTRAN EXPRESSIONS USED WHEN DETERMINING VELOCITIES

The Fortran expressions used to compute both mean-flow and turbulent velocities in the Airwake Module correspond to the mathematical equations given in Section 3. Velocities are computed using subroutines ENVIR and BURBLE.

A1.1 Subroutine ENVIR

Subroutine ENVIR computes both mean-flow and turbulent velocities for an ambient turbulent atmosphere.

Considering mean-flow velocities, these are denoted by VNW, VEW, and VDW, for the longitudinal, lateral, and vertical ship-coordinate directions respectively, and the relevant expressions used to determine these velocities are as follows:

```
      AFVWD = 1.688*AFVW
      AFWDR = 0.01745*AFPSIW
      VNW = -AFVWD*(COS(AFWDR))
      VEW = -AFVWD*(SIN(AFWDR))
      VDW = 0.0
```

Considering turbulent velocities, these are denoted by AFUTRB, AFVTRB, and AFWTRB for the longitudinal, lateral, and vertical ship-coordinate directions respectively, and the relevant expressions used to determine these velocities are as follows:

```
      AFWN1 = AFRN(1)*ABS(AFRN(1))*AFUSIG*AFTL
      AFWN2 = AFRN(2)*ABS(AFRN(2))*AFVSIG*AFTL
      AFGALT = 1.0
      IF(AFHGR.GT.100.0)GO TO 4050
      AFTEMP = 1.0
      AFGALT = 0.005*AFHGR+0.5
4050  AFWN3 = AFRN(3)*ABS(AFRN(3))*AFWSIG*AFTL*AFTEMP
      AFTGAIN = SQRT(0.01*AFVP)*AFGALT*DTENVIR
      AFLAGF = 1.0-DTENVIR*0.01*AFVP
      AFUTRB = AFUTRB*AFLAGF+AFWN1*AFTGAIN
      AFVTRB = AFVTRB*AFLAGF+AFWN2*AFTGAIN
      AFWTRB = AFWTRB*AFLAGF+AFWN3*AFTGAIN
```

A1.2 Subroutine BURBLE

Subroutine BURBLE computes an incremental flow field due to the presence of the ship for both mean-flow and turbulent velocities.

Mean-flow velocities are denoted by ARUS1, ARVS1, and ARWS1 for the longitudinal, lateral, and vertical ship-coordinate directions respectively. Corresponding turbulent velocities are denoted by ARUTL, ARVTL, and ARWTL respectively. The mean-flow and turbulent velocities are used to determine the incremental burble velocities which are denoted by ARUSWND, ARVSWND, and ARWSWND respectively. Relevant expressions used to determine these velocities are as follows:

```
ARVXB = ARBWO*(ARVXXZ*ARKVXY*ARKXWOD+ARDXWOD)
ARVYB = ARBWO*(ARVYXZ*ARKVYY*ARKYWOD+ARDYWOD)
ARVZB = ARBWO*(ARVZXZ*ARKVZY*ARKZWOD+ARDZWOD)
ARTLB = ARBWO*(ARTLXZ*ARKTLY*ARKTWOD+ARDTWOD)
ARTEMP = (ARPSI+ARWODD)*0.01745
ARUS1 = ARWOD*1.688*(ARVXB*COS(ARTEMP)+ARVYB*SIN(ARTEMP))
ARVS1 = ARWOD*1.688*(ARVYB*COS(ARTEMP)-ARVXB*SIN(ARTEMP))
ARWS1 = ARWOD*1.688*ARVZB
ARTL1 = ARWOL 1.688*ARTLB*AFTGAIN
ARLAGF = 1.0-DTBURB*0.01*AFVP
ARWN1 = AFRN(1)*AZRAND1*AFUSIG*ARTL
ARWN2 = AFRN(2)*AZRAND2*AFVSIG*ARTL
ARWN3 = AFRN(3)*AZRAND3*AFWSIG*ARTL
ARUTL = ARUTL*ARLAGF+ARWN1*ARKTLU*ARTL1
ARVTL = ARVTL*ARLAGF+ARWN2*ARKTLV*ARTL1
ARWTL = ARWTL*ARLAGF+ARWN3*ARKTLW*ARTL1
ARUSWND = (ARUS1+ARUTL)*ARKXL+ARUSWND*(1.-ARKXL)
ARVSWND = (ARVS1+ARVTL)*ARKXL+ARVSWND*(1.-ARKXL)
ARWSWND = (ARWS1+ARWTL)*ARKXL+ARWSWND*(1.-ARKXL)
```

DISTRIBUTION

DSTO-TR-0015

AUSTRALIA

DEFENCE ORGANISATION

Defence Science and Technology Organisation

Chief Defence Scientist
FAS Science Policy
AS Science Corporate Management
} shared copy

Counsellor, Defence Science, London (Doc Data Sheet only)
Counsellor, Defence Science, Washington (Doc Data Sheet only)
Office of Naval Attache, Washington
Senior Defence Scientific Adviser (Doc Data Sheet only)
Scientific Adviser Policy and Command (Doc Data Sheet only)
Navy Scientific Adviser
Scientific Adviser - Army (Doc Data Sheet only)
Air Force Scientific Adviser (Doc Data Sheet only)
Director Trials
Main Library - DSTO Salisbury
Aeronautical and Maritime Research Laboratory
- Director
- Library Fishermens Bend
- Library Maribyrnong
- Chief - Air Operations Division
- Chief - Airframes and Engines Division
- Research Leader - Aircraft Performance
- Research Leader - Flight Systems
- Head - Helicopter Operations (6 copies)
- Author: L.P. Erm (5 copies)
- B.D. Forrester
- D.J. Sherman
- J.F. Harvey
- N. Matheson
- B. Phelps Maribyrnong

Defence Central

OIC TRS, Defence Central Library
Document Exchange Centre, DIS (8 copies)
Defence Intelligence Organisation
Library, Defence Signals Directorate (Doc Data Sheet only)

Navy

Aircraft Maintenance and Flight Trials Unit
Director of Aircraft Engineering - Navy
Superintendent Naval Aircraft Logistics
Director of Aviation Projects - Navy

Army

Engineering Development Establishment, Library

Air Force

OIC ATF, ATS, RAAFSTT, WAGGA (2 copies)
Aircraft Research and Development Unit
Scientific Flight Group
Library

UNIVERSITIES AND COLLEGES

Australian Defence Force Academy
Library
Head of Aerospace and Mechanical Engineering

OTHER ORGANISATIONS

NASA (Canberra)
AGPS

CANADA

Defence Research Establishment, Atlantic
J.L. Colwell
National Research Council, Ottawa
M. Sinclaire (Canadian NL TTCP HTP-6)
S. Zan
University of Toronto
L.D. Reid
Bombardier Inc., Canadair, Montreal
B.I.K. Ferrier

UNITED KINGDOM

Defence Research Agency, Bedford
G.D. Padfield
S. Tate
B. Tomlinson
Defence Research Agency, Farnborough
A.F. Jones (UKNL TTCP HTP-6)

UNITED STATES

US Army Aeroflightdynamics Directorate, Ames Research Center
W.G. Bousman (USNL TTCP HTP-6)
Naval Air Warfare Center, Aircraft Division, Warminster
J.W. Clark, Jr (TTCP HTP-6)
J. Funk
Naval Air Warfare Center, Aircraft Division, Patuxent River
D. Carico
J. McCrillis
L. Trick
Naval Air Warfare Center, Aircraft Division, Lakehurst
H. Fluk
Georgia Institute of Technology, Atlanta
D. Mavris

SPARES (10 copies)

TOTAL (79 copies)

AL 149 DEPARTMENT OF DEFENCE

DOCUMENT CONTROL DATA

PAGE CLASSIFICATION
UNCLASSIFIED

PRIVACY MARKING

1a. AR NUMBER	1b. ESTABLISHMENT NUMBER	2. DOCUMENT DATE	3. TASK NUMBER
AR-008-644	DSTO-TR-0015	MAY 1994	AO/MGT

4. TITLE

A PRELIMINARY STUDY OF THE AIRWAKE MODEL USED IN AN EXISTING SH-60B/FFG-7 HELICOPTER/SHIP SIMULATION PROGRAM

5. SECURITY CLASSIFICATION (PLACE APPROPRIATE CLASSIFICATION IN BOX(S) IE. SECRET (S), CONF. (C) RESTRICTED (R), LIMITED (L), UNCLASSIFIED (U)).

DOCUMENT	TITLE	ABSTRACT
U	U	U

6. NO. PAGES 38

7. NO. REFS. 19

8. AUTHOR(S)

Lincoln P. Erm

9. DOWNGRADING/DELIMITING INSTRUCTIONS

Not applicable.

10. CORPORATE AUTHOR AND ADDRESS

AERONAUTICAL AND MARITIME RESEARCH LABORATORY

AIR OPERATIONS DIVISION

506 LORIMER STREET

FISHERMENS BEND VIC 3207

11. OFFICE/POSITION RESPONSIBLE FOR:

SPONSOR NAVY

SECURITY -

DOWNGRADING -

APPROVAL CAOD

12. SECONDARY DISTRIBUTION (OF THIS DOCUMENT)

Approved for public release.

OVERSEAS ENQUIRIES OUTSIDE STATED LIMITATIONS SHOULD BE REFERRED THROUGH DSTIC, ADMINISTRATIVE SERVICES BRANCH, DEPARTMENT OF DEFENCE, ANZAC PARK WEST OFFICES, ACT 2601

13a. THIS DOCUMENT MAY BE ANNOUNCED IN CATALOGUES AND AWARENESS SERVICES AVAILABLE TO ....

No limitations

14. DESCRIPTORS

Guided missile frigates
Helicopter wakes
Aerodynamic wakes
Velocity measurement
Wind tunnel tests
Simulation

15. DISCAT SUBJECT CATEGORIES

010301
1402

16. ABSTRACT

The ship airwake model in a SH-60B/FFG-7 helicopter/ship simulation program is studied in detail. The airwake model is based on wind tunnel measurements obtained for another ship type, with geometric scaling applied to make it suitable for an FFG-7 frigate. Velocities over the flight deck of an FFG-7, predicted using the program, are compared with those obtained from full-scale tests on HMAS Darwin. Differences between predicted and measured velocities are often found to occur, indicating that the model used for prediction should be based on measurements for an FFG-7.

PAGE CLASSIFICATION
UNCLASSIFIED
PRIVACY MARKING

THIS PAGE IS TO BE USED TO RECORD INFORMATION WHICH IS REQUIRED BY THE ESTABLISHMENT FOR ITS OWN USE BUT WHICH WILL NOT BE ADDED TO THE DISTS DATA UNLESS SPECIFICALLY REQUESTED.

16. ABSTRACT (CONT).

17. IMPRINT

AERONAUTICAL AND MARITIME RESEARCH LABORATORY, MELBOURNE

18. DOCUMENT SERIES AND NUMBER	19. WA NUMBER	20. TYPE OF REPORT AND PERIOD COVERED
DSTO Technical Report 0015	76 000B	

21. COMPUTER PROGRAMS USED

22. ESTABLISHMENT FILE REF.(S)

M1/8/797

23. ADDITIONAL INFORMATION (AS REQUIRED)